Software for Modeling of Long-Term Growth of Bulk AlN Crystals by Physical Vapor Transport

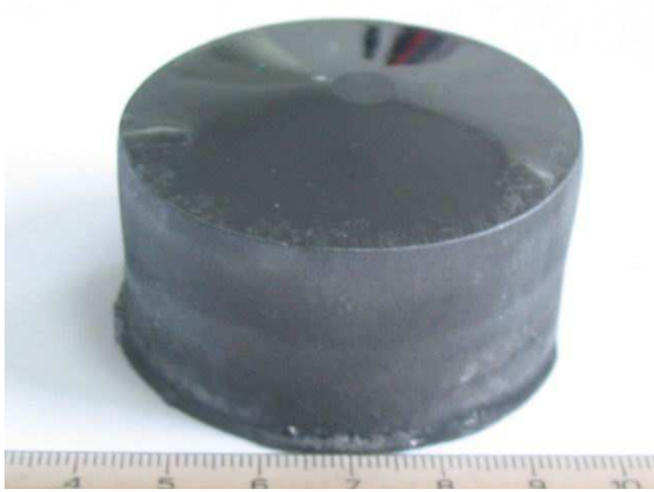

VR-PVT AlN

STR-Group Ltd

2014

STR Virtual Reactor (VR) is a **family** of stand-alone 2D software tools designed for the simulation of long-term growth of bulk crystals and epilayers from vapor

Virtual Reactor editions:

Physical Vapor Transport

- For growth of SiC: **VR-PVT SiC**
- For growth of AlN: **VR-PVT AlN**

Hydride Vapor Phase Epitaxy: HEpiGaNS

- For growth of **GaN**
- For growth of **AlN** and **AlGaN**

Chemical Vapor Deposition

- For growth of SiC: **VR-CVD SiC**

VR-PVT AlN — Key Features

- VR-PVT AlN is specially designed for the modeling of long-term AlN bulk crystal growth by the seeded sublimation technique
- Account of non-steady character of the growth process (crystal enlargement, heater or crucible movement, etc.)
- Modeling of the heat transfer in the overall growth system
- Modeling of multicomponent flow
- Modeling of diffusion of the reactive species in the growth chamber
- Advanced models of heterogeneous chemical reactions
- Prediction of material losses
- Estimation of the internal pressure inside the crucible
- Analysis of dislocation evolution
- Analysis of heat and mass transport in the porous source

Global Heat Transfer in an AlN Growth System

- Heat transfer mechanisms
  - Heat conduction in anisotropic media
  - Radiation
  - Convection
- RF heating with non-uniform heat distribution in the crucible by a single coil or two independent coils
- Heat transfer in porous source
- Heat transfer in thermal insulation
- Temperature fitting at a reference point

Simulation of the Heat Transfer in Porous AlN Source

Virtual Reactor employs an advanced model of the heat transfer in porous media

Key Features

- Heat conduction through the granule contact spots
- Radiation transport though the pores
- Radiation transport through the granules

E.L. Kitanin et al., Mat. Sci. Engng. B55 (1998) 174

Temperature Distribution in an AlN Growth System

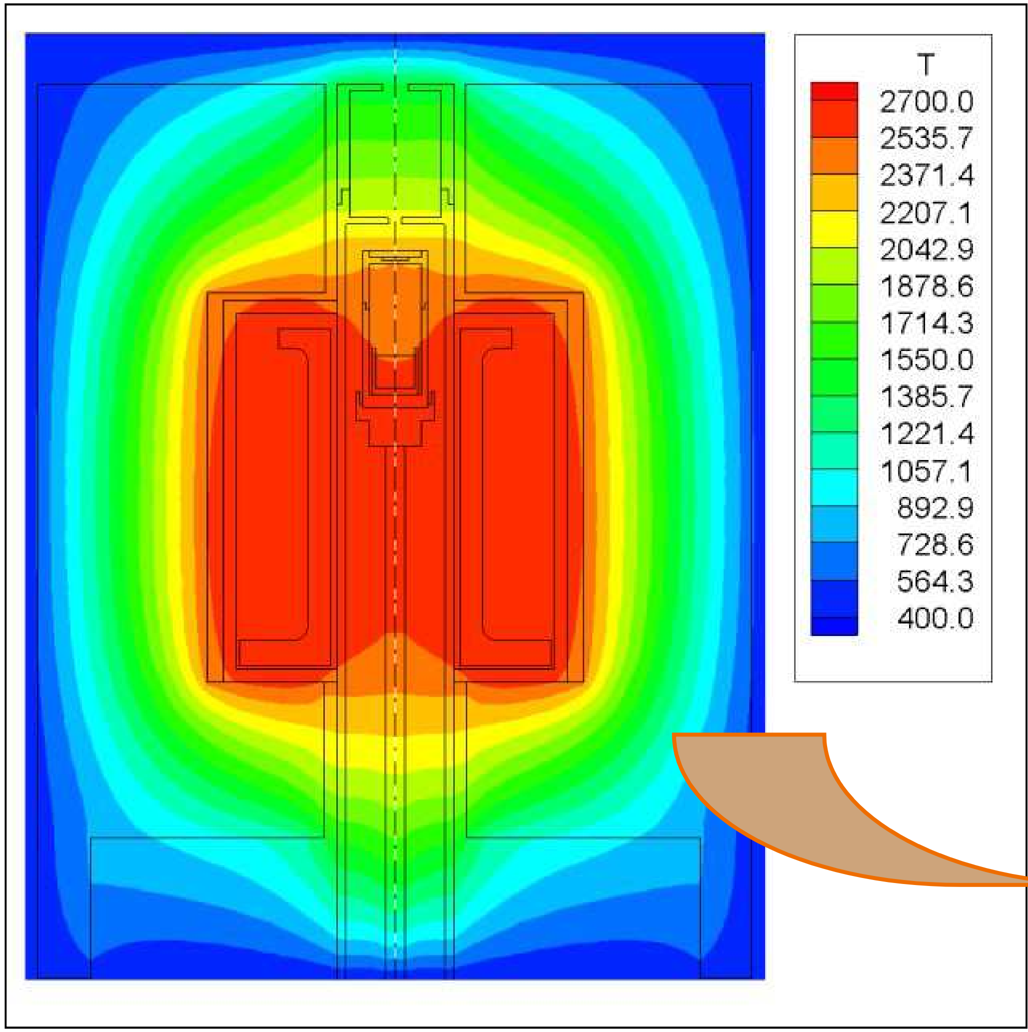

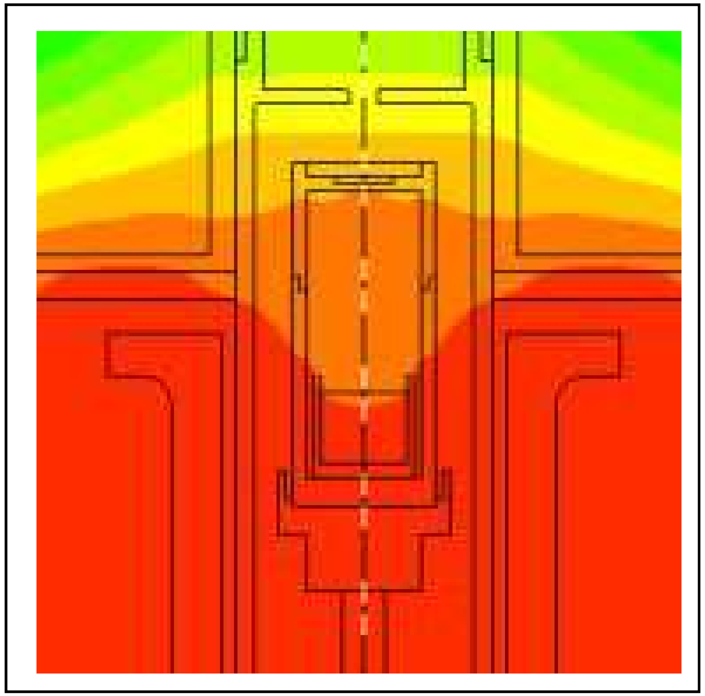

M.V. Bogdanov et al,
Mat. Res. Soc. Proc. 743
(2003) L3.33

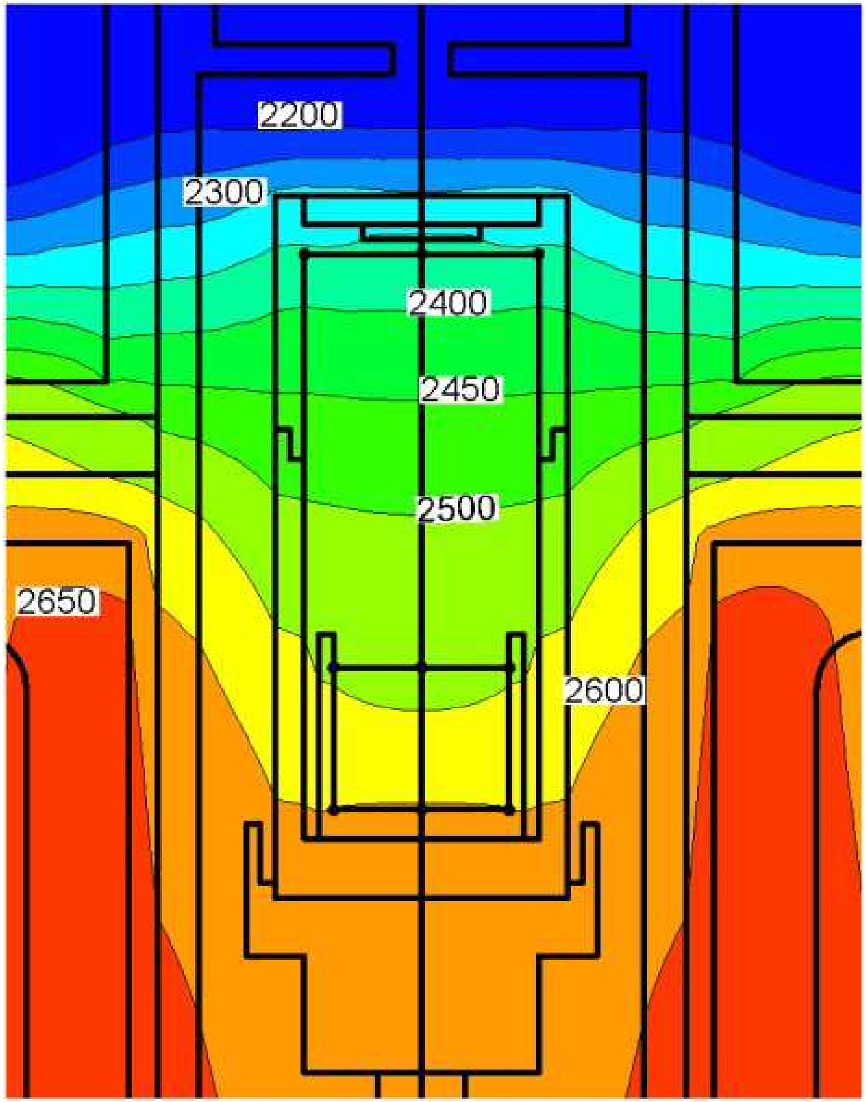

Temperature Distribution in the Crucible

M.V. Bogdanov et al,
Mat. Res. Soc. Proc. 743
(2003) L3.33

Modeling of Species Transport in AlN Crystal Growth

Use of the advanced models of species transport and heterogeneous processes in the sublimation growth of bulk AlN crystals

Employment of the material database containing accurate data on materials thermal conductivity

Mechanisms of Bulk AlN Crystal Growth

- Multicomponent vapor flow
- Diffusion of reactive species
- Heterogeneous reactions on the seed and source surfaces
- Stefan flow
- Mass exchange between the growth cell and the ambient

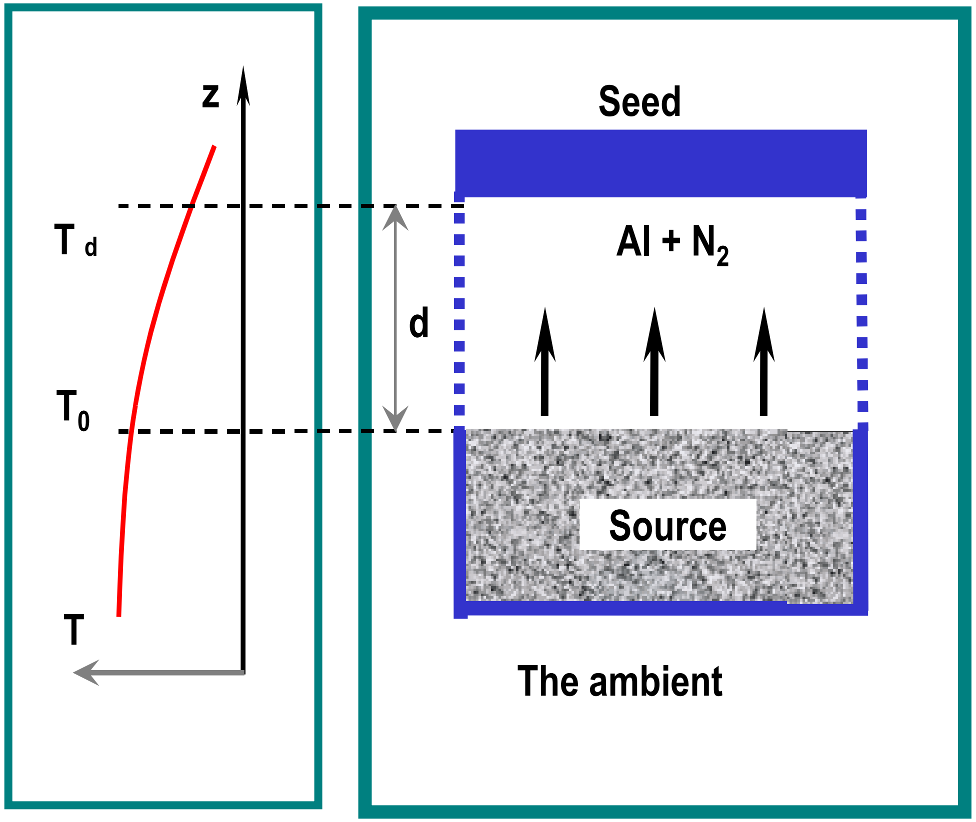

Quasi-Thermodynamic Approach

VR employs the quasi-thermodynamic model for the description of heterogeneous processes

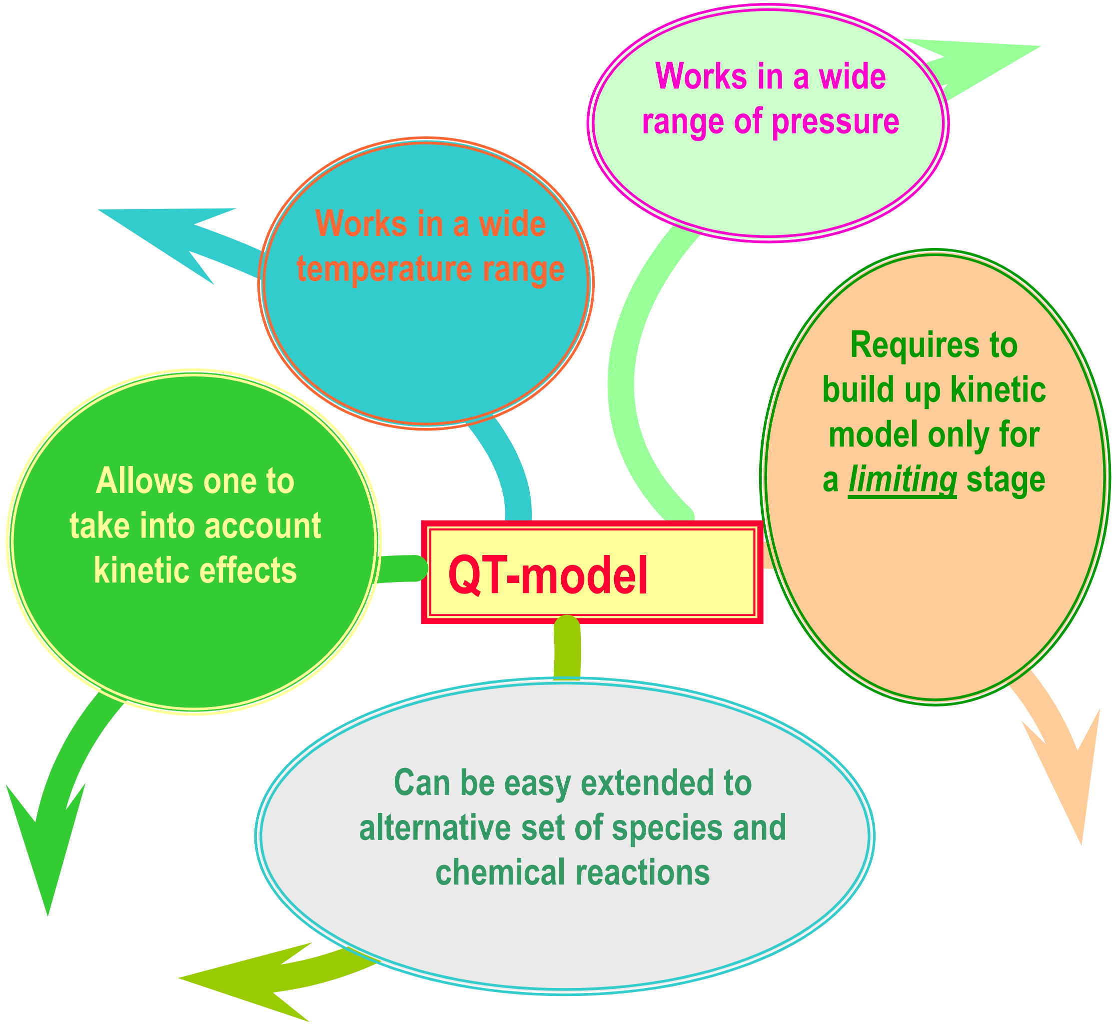

S.Yu. Karpov et al.,
MRS Int. J. Nitr. Sem. Res. 4 (1999) 4

A.S.Segal et al,
J. Crystal Growth 211 (2000) 68

Basic Assumptions

- Gaseous species: **Al**, $\mathbf{N_2}$
- Reaction: $\mathbf{2\ Al + N_2 = 2\ AlN}$ (solid)
- The atoms in the adsorption layer are nearly in thermodynamic equilibrium with the crystal: atom incorporation and desorption rates are much higher than their difference, i.e. the crystal growth rate
- Kinetics effects at the adsorption /desorption stages are accounted for by sticking/evaporation coefficients of the species

Species molar fluxes:

$$J_i = \beta_i \left(p_i - p_i^0 \right)$$

i = Al, N_2

$$\beta_i = \sqrt{\frac{1}{2\pi M_i RT}}$$ - the Hertz-Knudsen factor

p_i - i-th species partial pressure

p_i^0 - i-th species equilibrium pressure

Mass action law for the equilibrium pressures:

$$\left(p_{Al}^0 \right)^2 p_{N_2}^0 = K(T)$$

$K(T)$ - equilibrium constant

Stoichiometric incorporation:

$$J_{Al} = 2J_{N_2} = \frac{\rho_{cr}}{M_{cr}} V_{gr}$$

ρ_{cr} - crystal density

M_{cr} - crystal molar mass

V_{gr} - growth rate

Adsorption Kinetics on AlN Surfaces

Aluminum adsorption kinetics:

$$\alpha_{Al} = 1$$

Nitrogen adsorption kinetics:

$$\alpha_{N_2} = \frac{3.5 e^{-\frac{30000}{T}}}{1.0 + 8 \cdot 10^{-15} e^{\frac{55000}{T}}}$$

S.Yu. Karpov et al.,
Phys. Stat. Sol. (a) 188 (2001) 763.

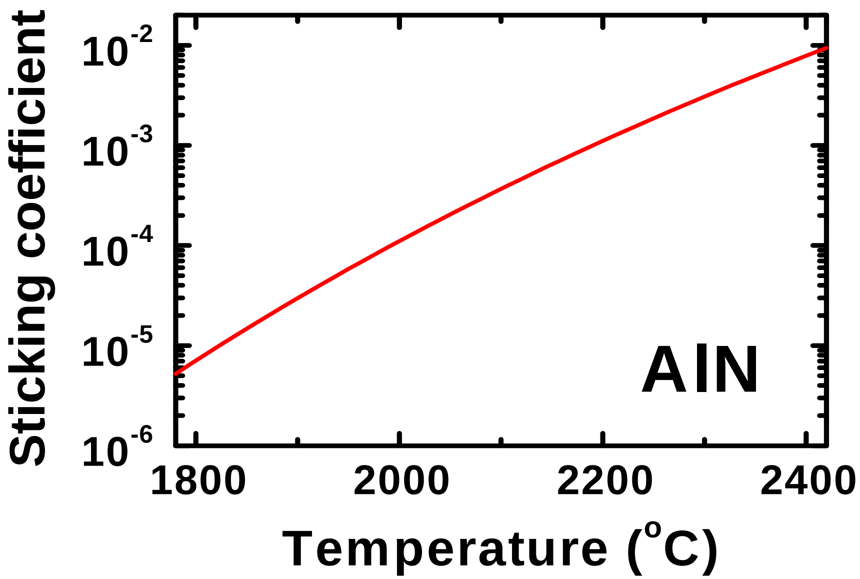

AlN Growth in the Nitrogen Atmosphere

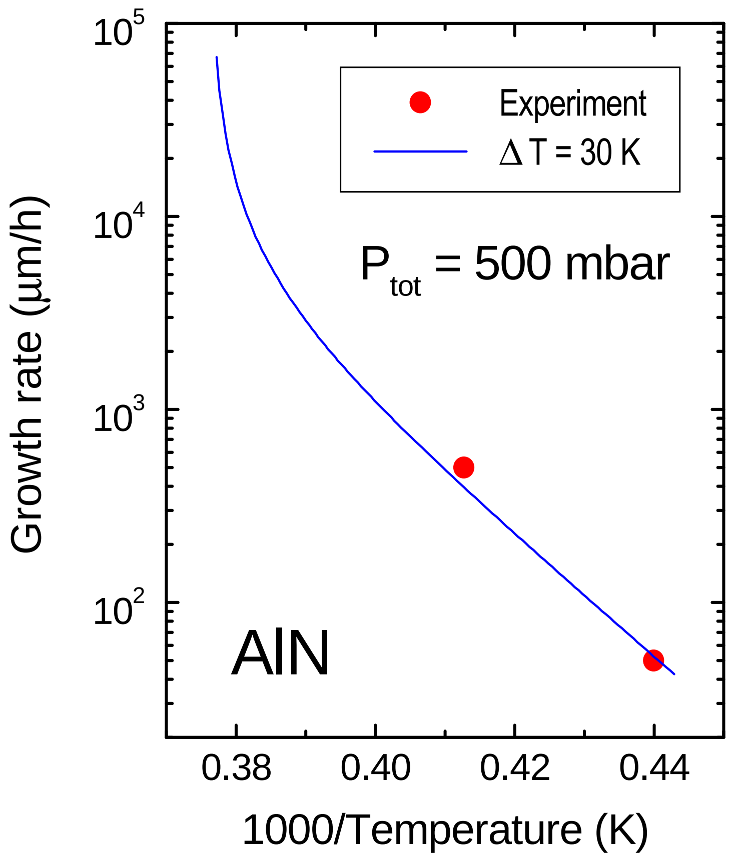

Experiments:
C.M. Balkas et al,
Mat. Res. Sos. Symp. Proc.
449 (1997) 41.

AlN Growth in the Nitrogen Atmosphere

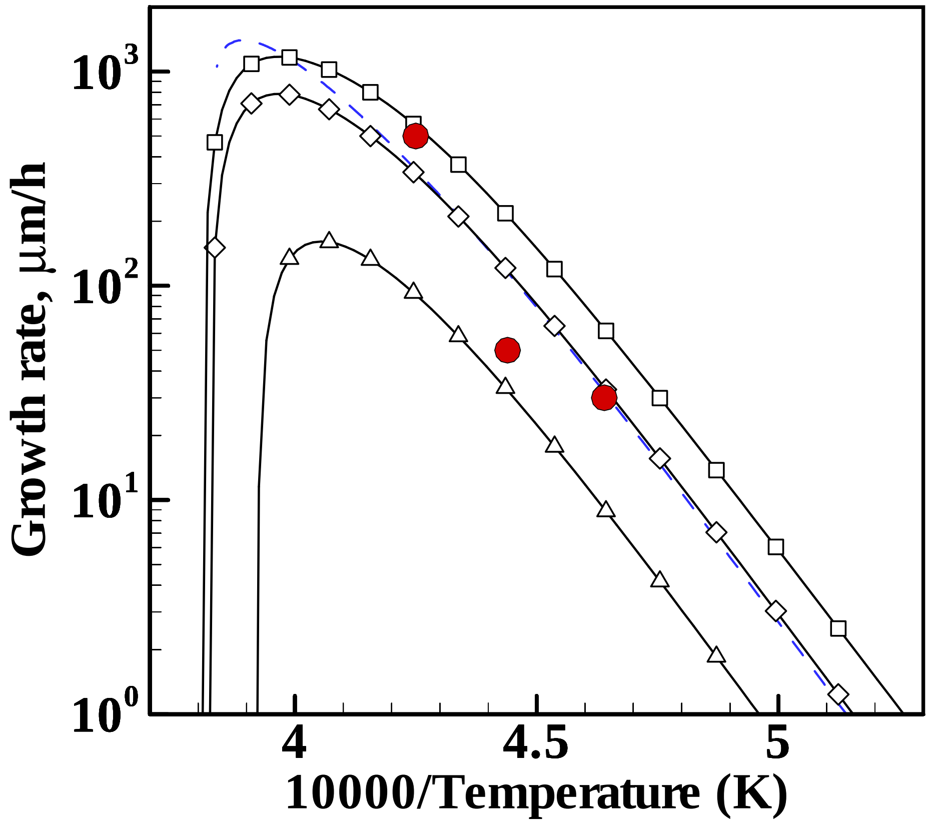

Solid circles: experimental data obtained at ΔT = 70 K

Solid curves - computations accounting for the mass exchange with the external ambient for different ΔT:

- Squares: ΔT = 100 K
- Diamonds: ΔT = 70 K
- Triangles: ΔT = 30 K

Dashed curve: theoretical predictions of the model for ΔT = 70 K

Experiments:
C.M. Balkas et al,
Mat. Res. Sos. Symp. Proc. 449 (1997) 41.

Growth Rate Limitation by the N_2 Adsorption Kinetics

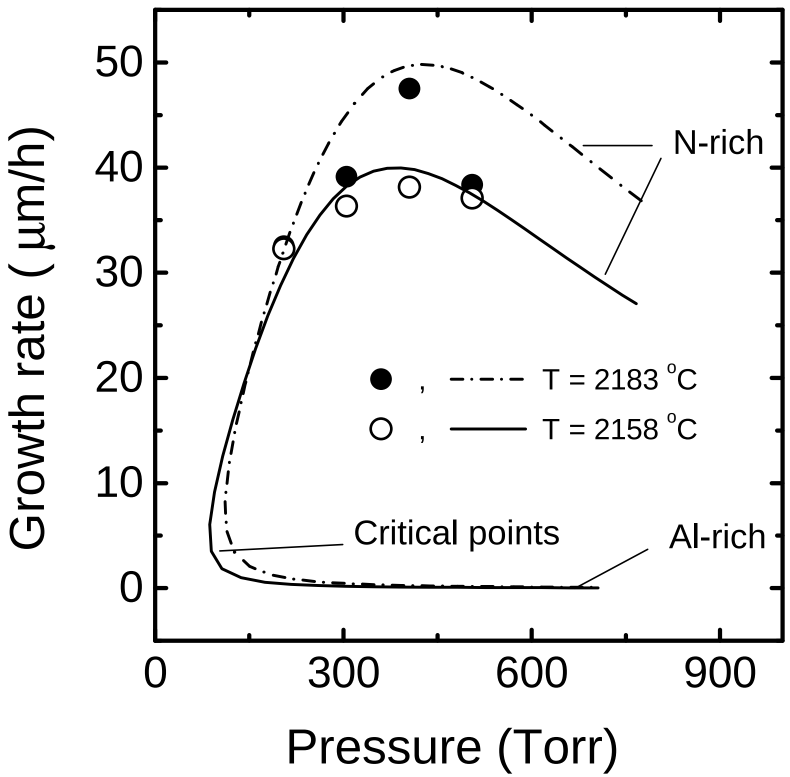

Computed and experimental AlN growth rates as a function of pressure at 2158°C and 2183°C. The clearance between the source and seed and the respective temperature difference are 4 mm and 4.5°C.

Experimental data obtained by M. Spencer

Growth Rate vs. Seed Temperature

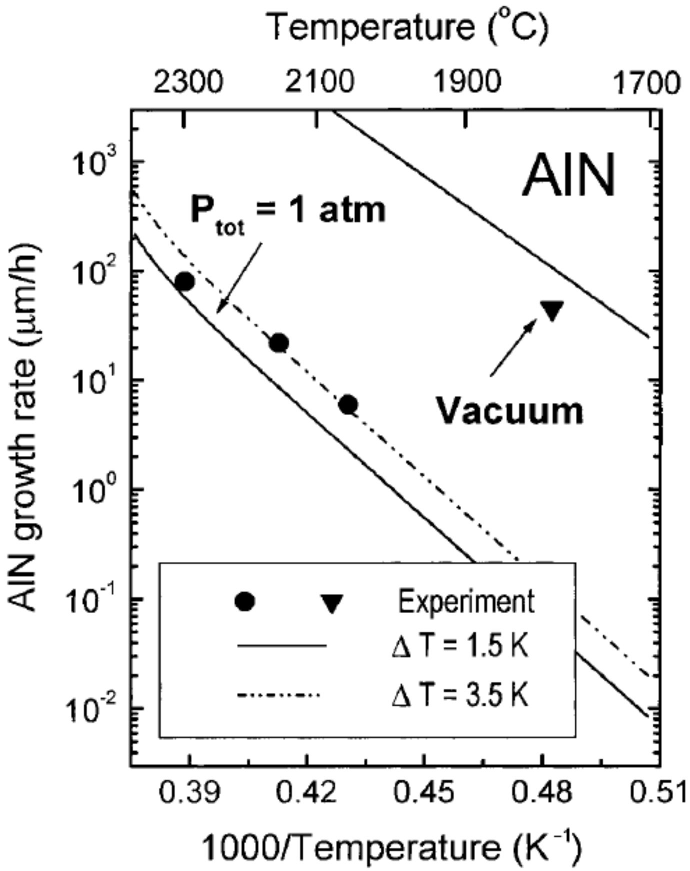

Computed and experimental AlN growth rates as a function of the seed temperature.
Clearance d = 4 mm

S.Yu. Karpov et al.,
Phys. Stat. Sol. (a) 176 (1999) 435.

AlN Growth Rate at Different Growth Stages

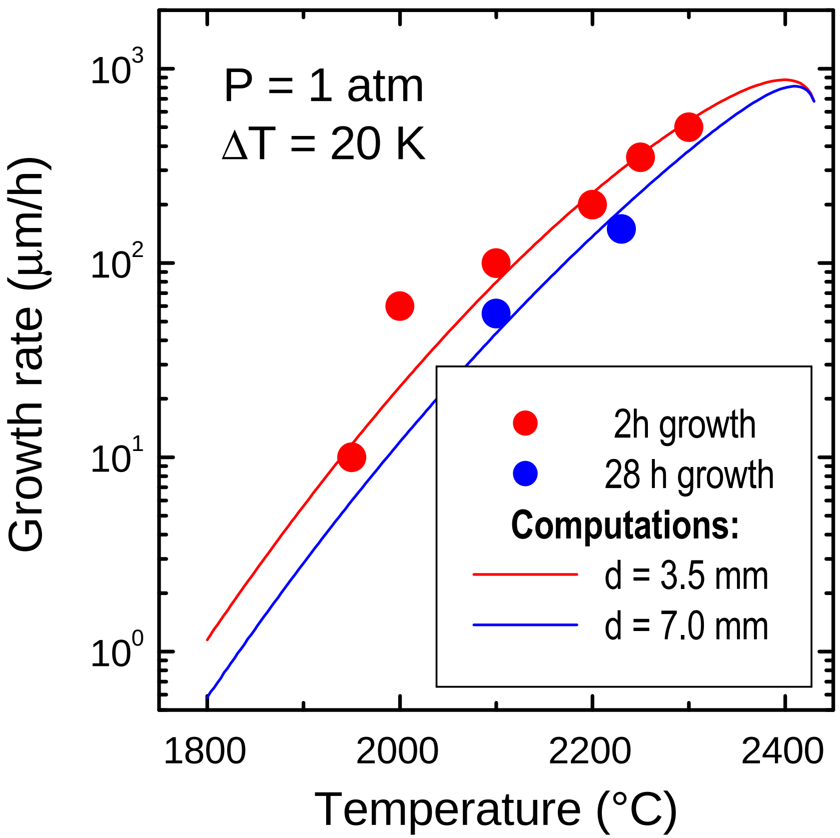

Circles: experiments
Lines: computations

E.N. Mokhov et al,
Mat. Sci. Forum 433-436
(2003) 979

Growth Rate vs. Seed Temperature

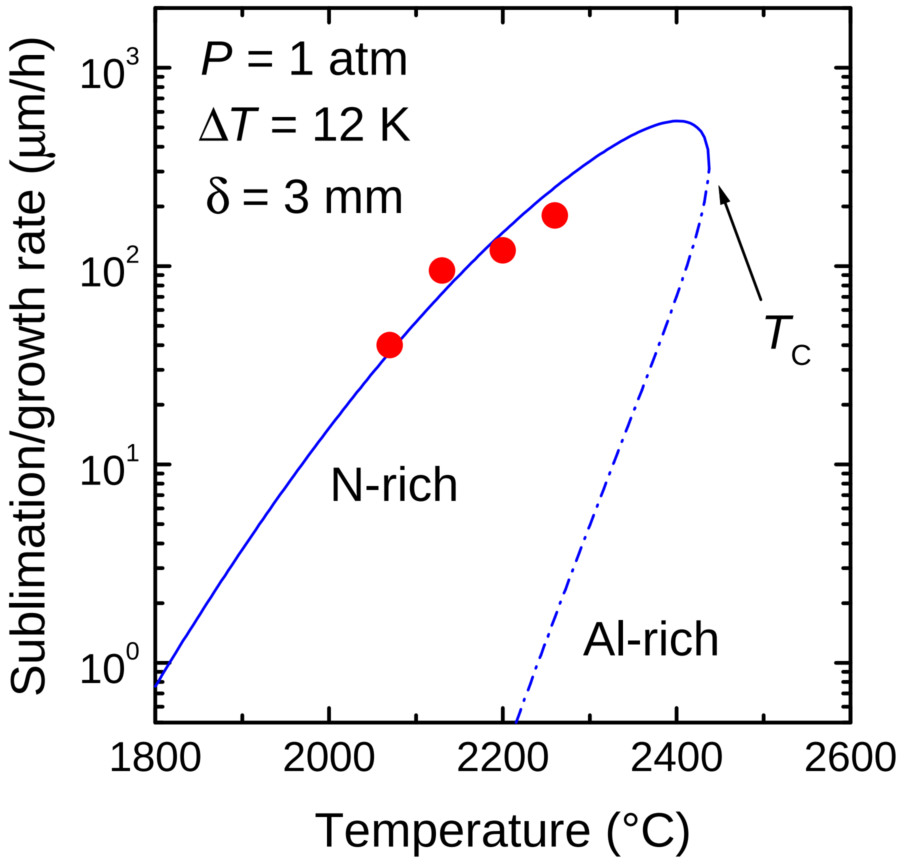

Circles: experiments
Lines: computations

S.Yu. Karpov et al,
Mat. Sci. Forum 353-356
(2001) 779

Experimental data by
Yu.A. Vodakov et al.

Growth of AlN Close to Critical Pressure

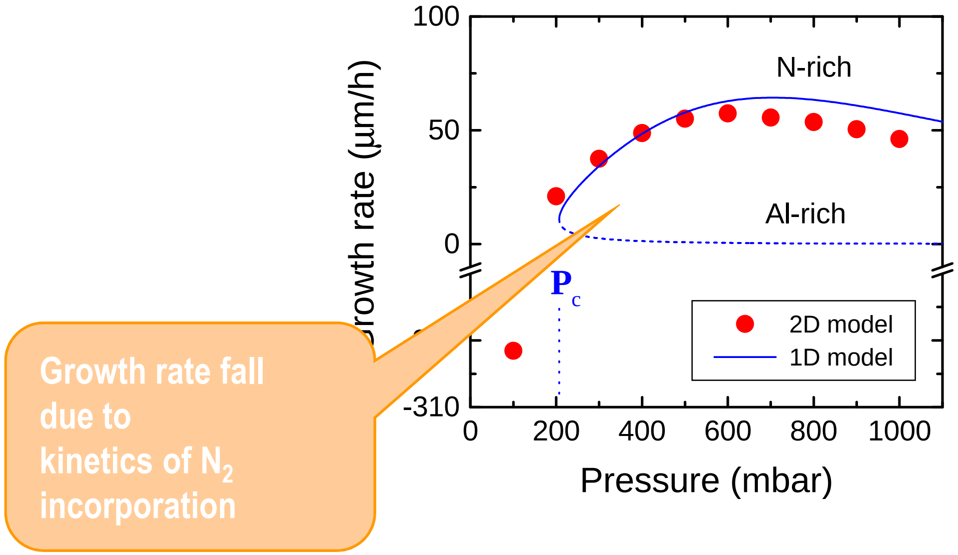

Comparison of
1D and 2D Computations

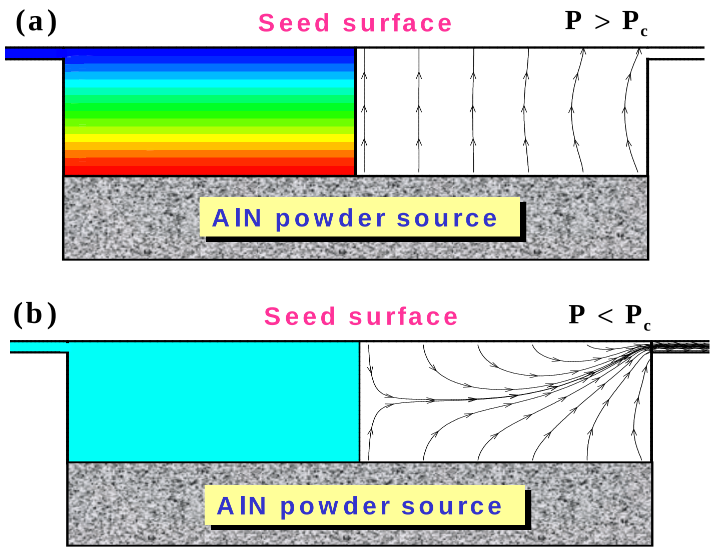

Gas flow (right) and
Al distribution (left)

S.Yu. Karpov et al, Mat. Sci. Forum 353-356 (2001) 779
Experimental data by Yu.A. Vodakov et al.

Flow Pattern and Species Distribution in the Growth Chamber

High pressure: P = 600 mbar

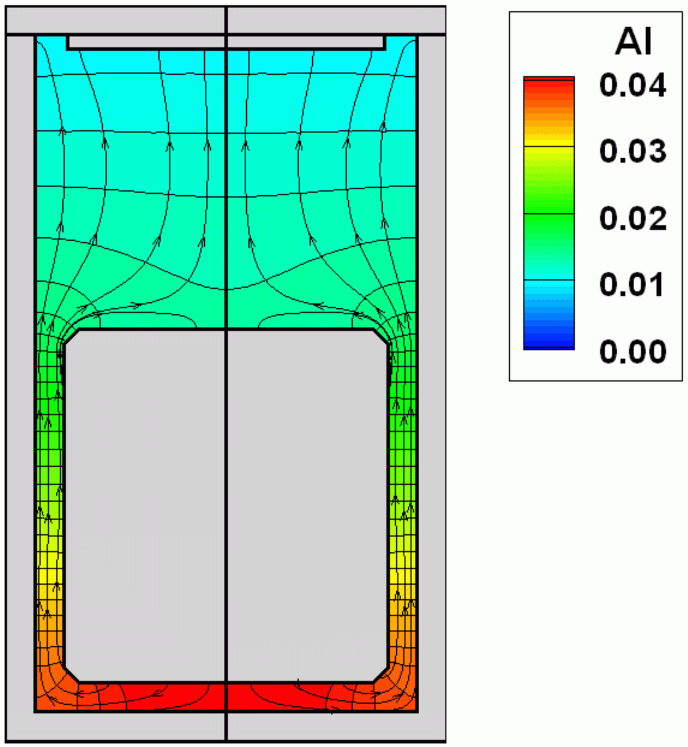

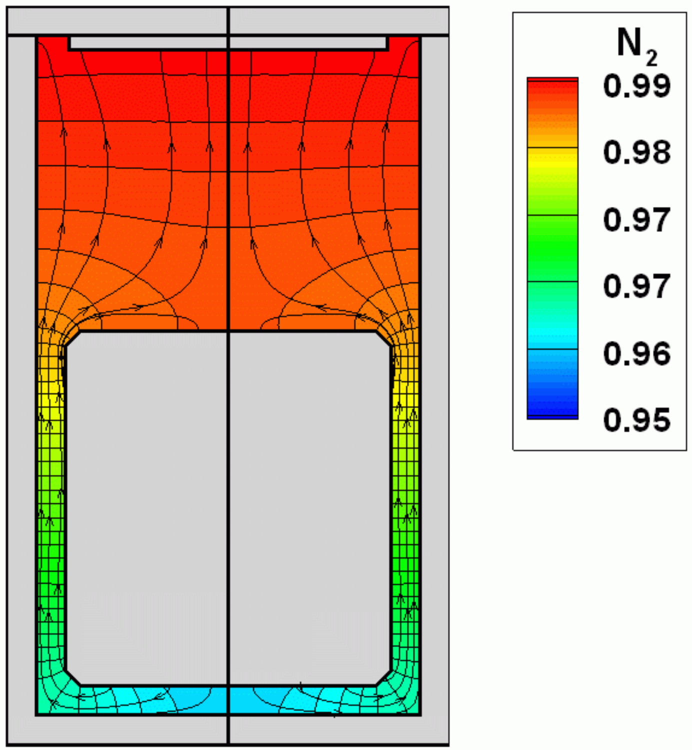

Flow Pattern and Species Distribution in the Growth Chamber

Medium pressure: P = 250 mbar

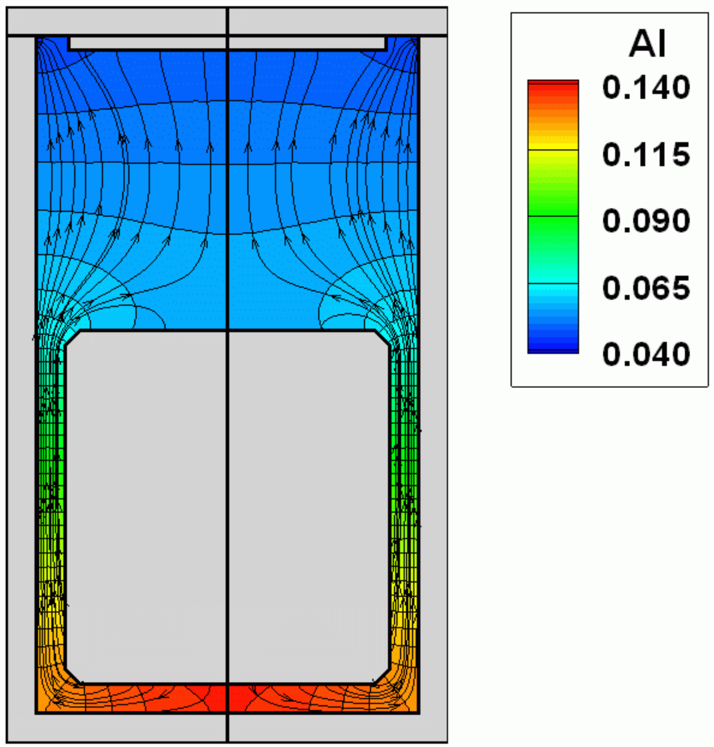

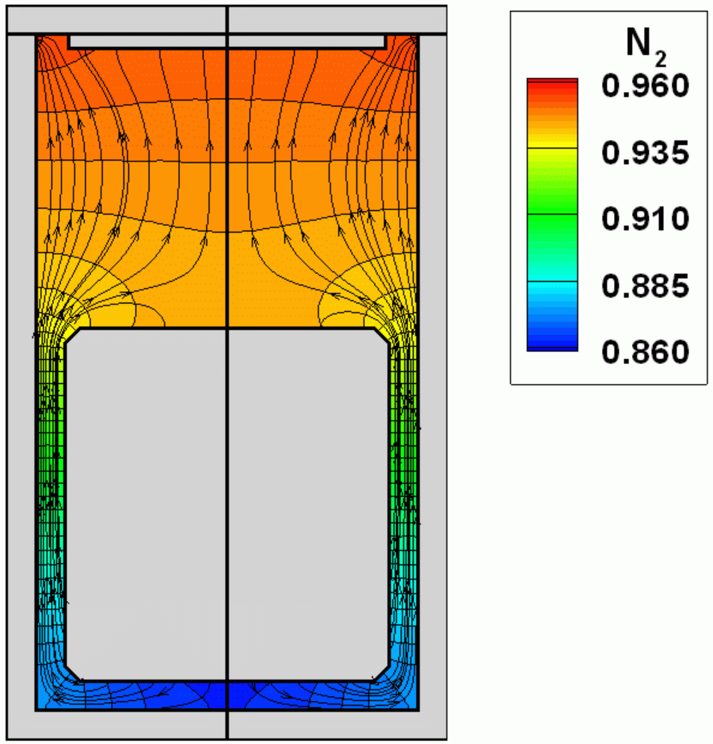

Flow Pattern and Species Distribution in the Growth Chamber

Very low pressure: P = 45 mbar

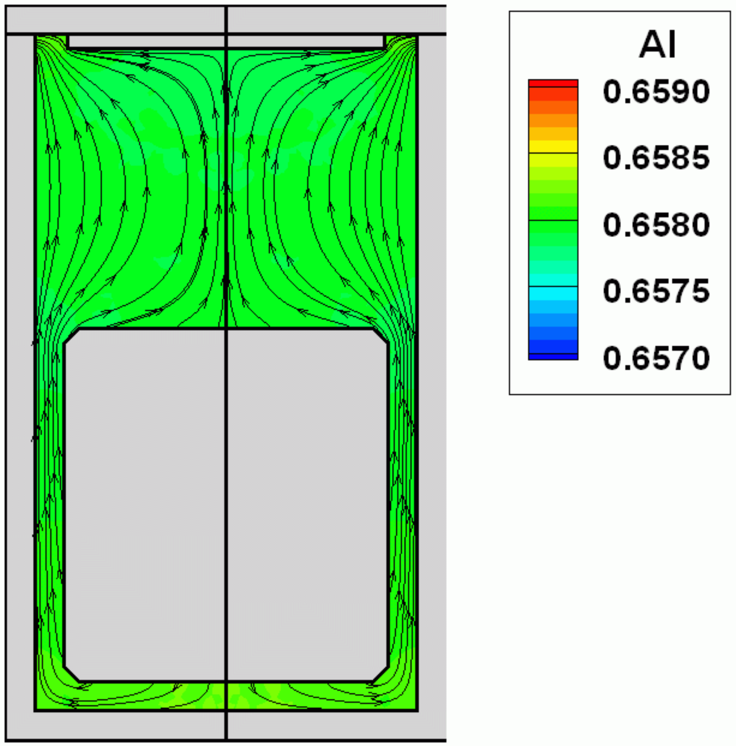

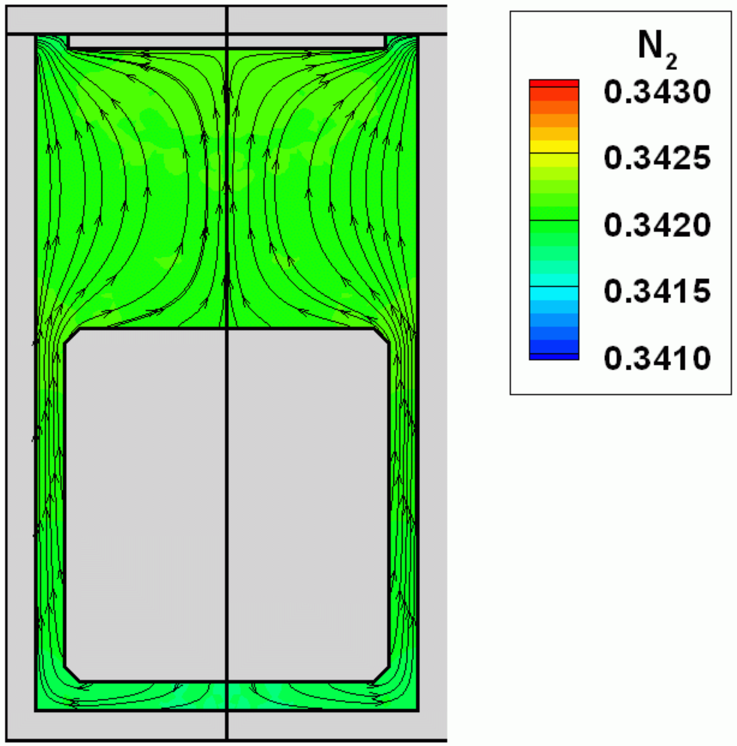

Simulation of Crystal Shape Evolution

Pressure = 600 mbar

Start of the growth

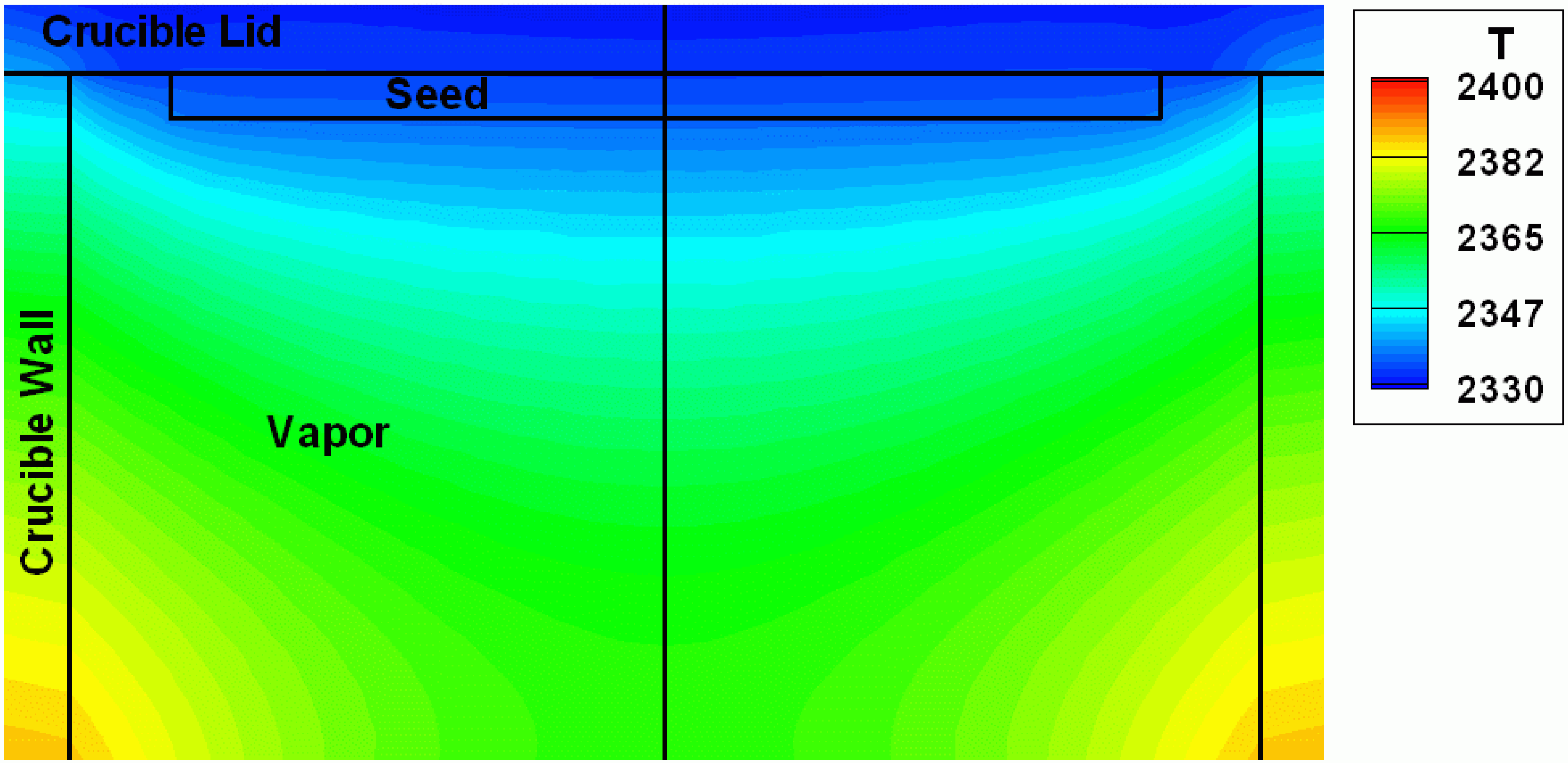

t = 5 h

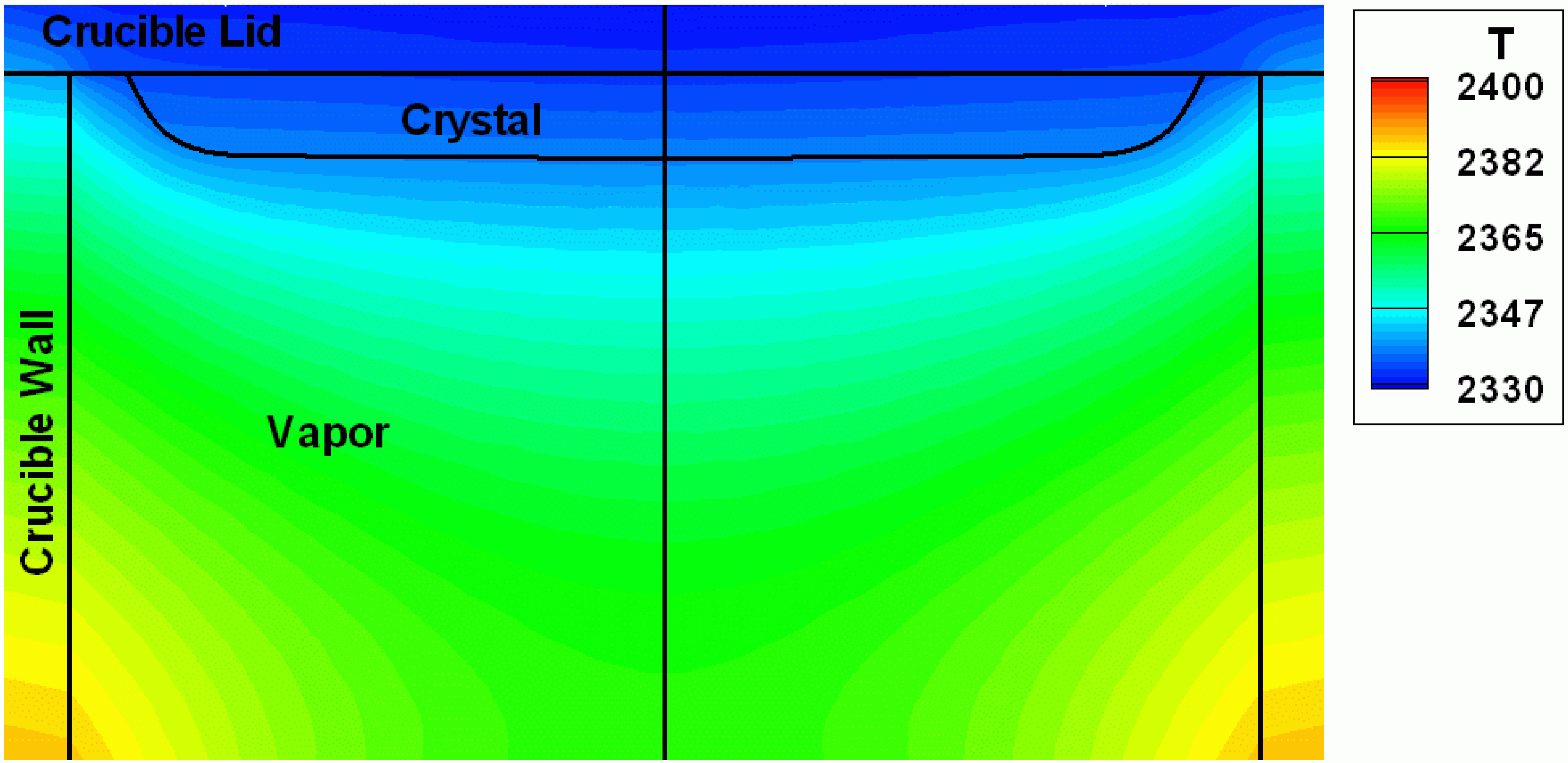
Crucible Lid
Crystal
Crucible Wall
Vapor
T
2400
2382
2365
2347
2330

t = 10 h

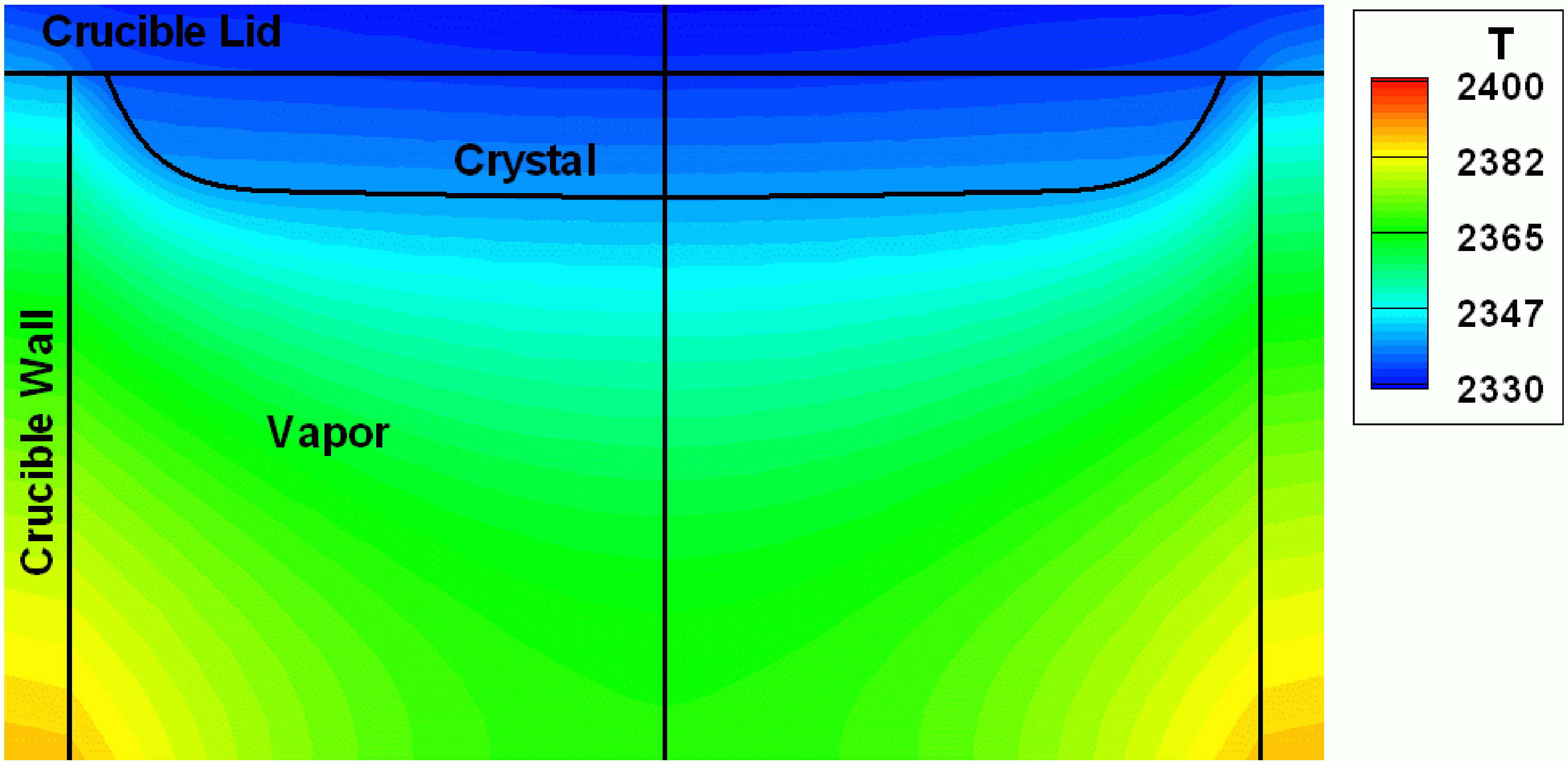
Crucible Lid
Crystal
Crucible Wall
Vapor
T
2400
2382
2365
2347
2330

t = 20 h

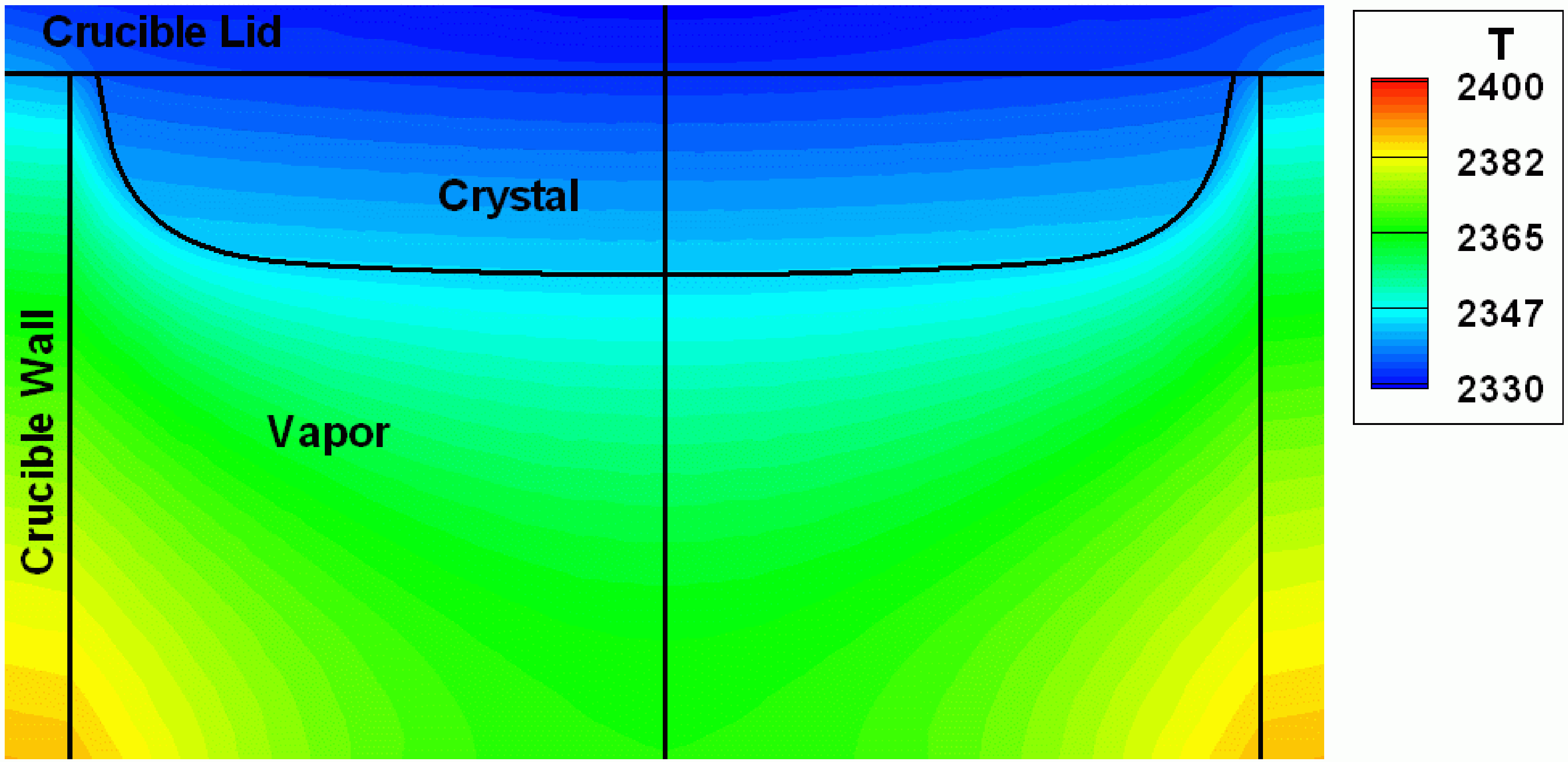
Crucible Lid
Crystal
Vapor
Crucible Wall
T
2400
2382
2365
2347
2330

t = 30 h

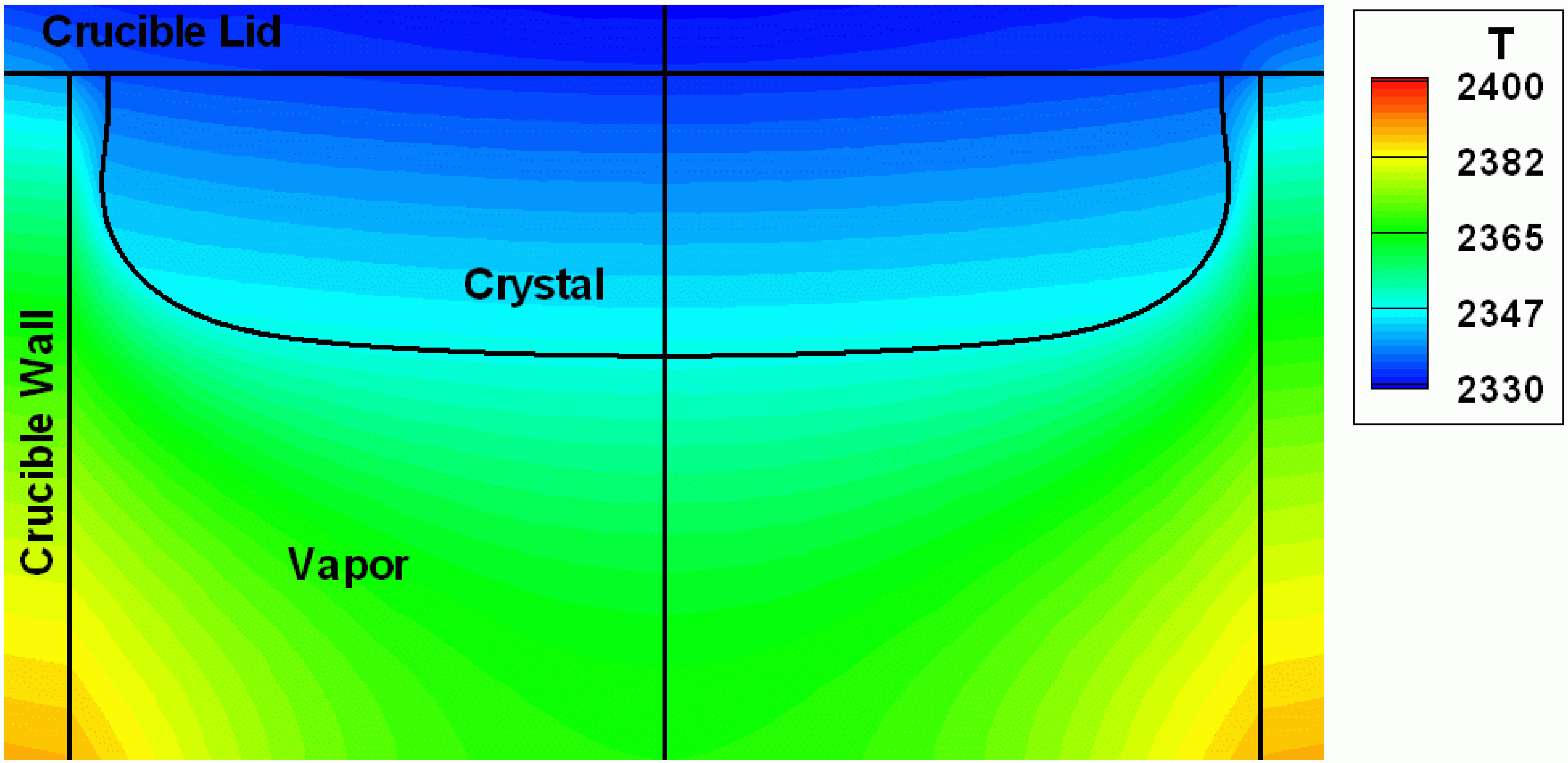
Crucible Lid
Crucible Wall
Crystal
Vapor
T
2400
2382
2365
2347
2330

t = 40 h

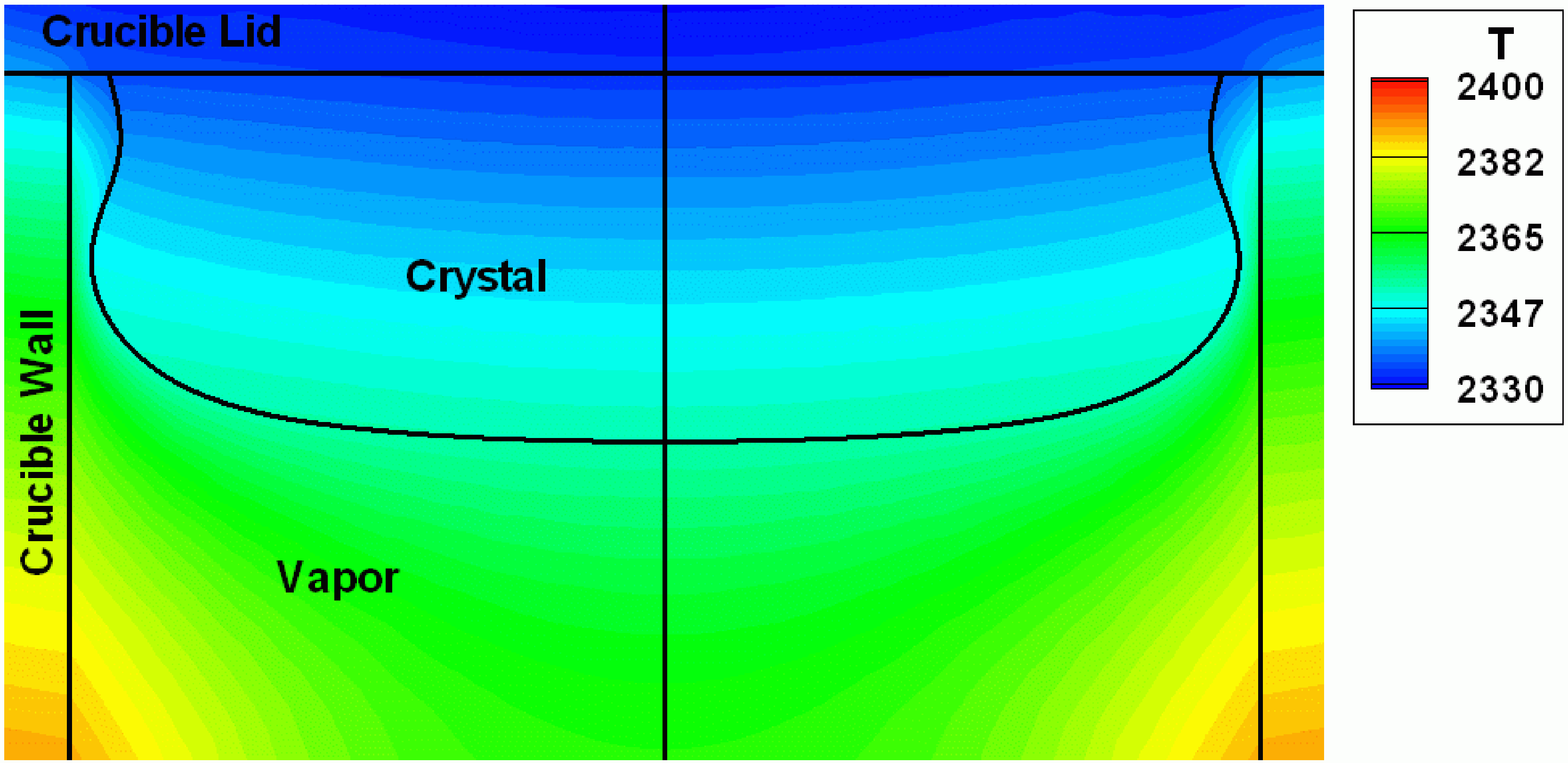
Crucible Lid
Crystal
Crucible Wall
Vapor
T
2400
2382
2365
2347
2330

t = 50 h

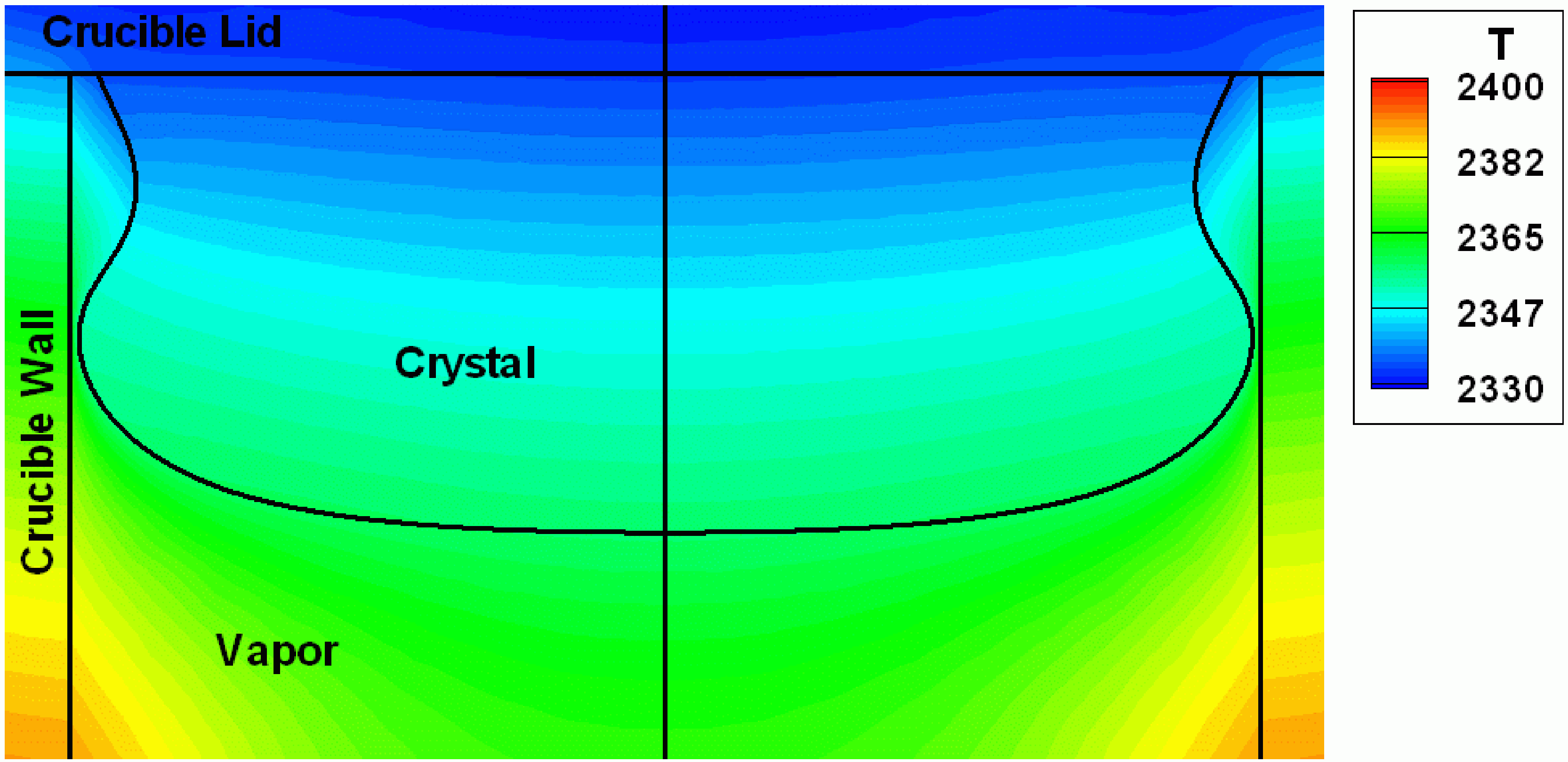
Crucible Lid
Crucible Wall
Crystal
Vapor
T
2400
2382
2365
2347
2330

Species Transport in the Porous Source

Processes Observed in the Porous Source during the Growth

- Complete evaporation of the hot zones
- Densification of the source in the cold zones along with the secondary crystallization from the supersaturated vapor
- Directional gas flow through the porous source. In particular, this results in modification of granule shapes due to their sublimation and secondary crystallization of the reactive species

Basic Concepts

- AlN source is considered as porous medium characterized by
  - Local porosity
  - Granule size
- Species transport in the source is modeled using the Darcy-Brinkman-Forchheimer approach
- The account of the volumetric mass source due to chemical reactions on the surface of AlN granules
- Temporal variation of the porosity and granule size due to granule sublimation and recrystallization

Governing Equations

The source porosity: $\varepsilon = \dfrac{V_{fluid}}{V_{cell}}$

The continuity equations for the whole vapor: $\nabla \cdot \left(\rho \vec{V}\right) = S^{m}$

The continuity equations for each species: $\nabla \cdot \left(\rho C_i \vec{V} + J_i\right) = S_i^{\,m}$

Flow in the porous medium is described by the Darcy-Brinkman-Forchheimer law:

$$\frac{1}{\varepsilon}\nabla \cdot \left(\frac{1}{\varepsilon}\rho \vec{V}\vec{V}\right) = -\nabla p - \frac{\mu}{K}\vec{V} + \nabla \cdot \tau - \frac{\rho C_F}{\sqrt{K}}\left|\vec{V}\right|\vec{V} - \rho \vec{g}$$

The porous medium permeability and inertial coefficient are found from the granule radius and porosity using Ergun's relationship:

$$K = \frac{4r^2\varepsilon^3}{150(1-\varepsilon)^2}$$

$$C_F = \frac{1.75}{\sqrt{150}}\varepsilon^{-3/2}$$

Boundary Conditions on the Source-Gas Interface:

The gas velocity: $\left.\vec{V}\right|_{b^-} = \left.\vec{V}\right|_{b^+}$

Pressure: $\left.p\right|_{b^-} = \left.p\right|_{b^+}$

Viscous stress tensor: $\left.\tau \cdot \vec{n}\right|_{b^-} = \left.\tau \cdot \vec{n}\right|_{b^+}$

Species: $\left.\left(\rho V_n C_i + J_i\right)\right|_{b^+} = \left.\left(\rho V_n C_i + J_i\right)\right|_{b^-}$

Modeling of the Porous Source Evolution

Temporal variation of the granule size:

$$\frac{dr}{dt} = -V_{subl}$$, where V_{subl} is the sublimation rate

Relationship between the porosity and the granule size:

$$\varepsilon = e^{-\eta}$$, where η is the reduced density defined as $$\eta = \frac{4}{3}\pi r^3 n_{gr}$$

The granule concentration assumed to be constant during the growth:

$$n_{gr} = -\frac{3\ln\varepsilon\big|_{t=0}}{4\pi\left(r\big|_{t=0}\right)^3}$$

Start of the growth

Initial porosity = 0.5

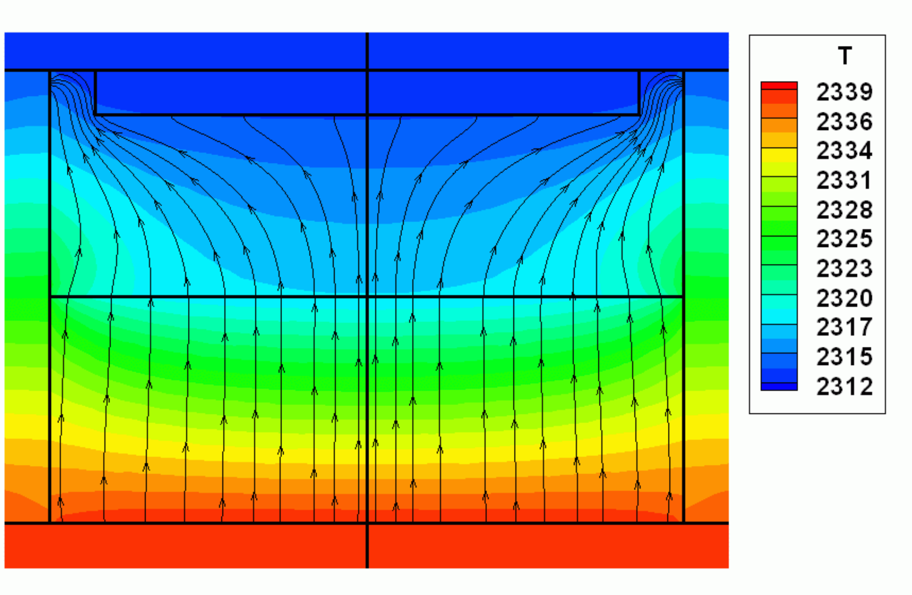

Temperature distribution and the
flow pattern
in the source and gas chamber

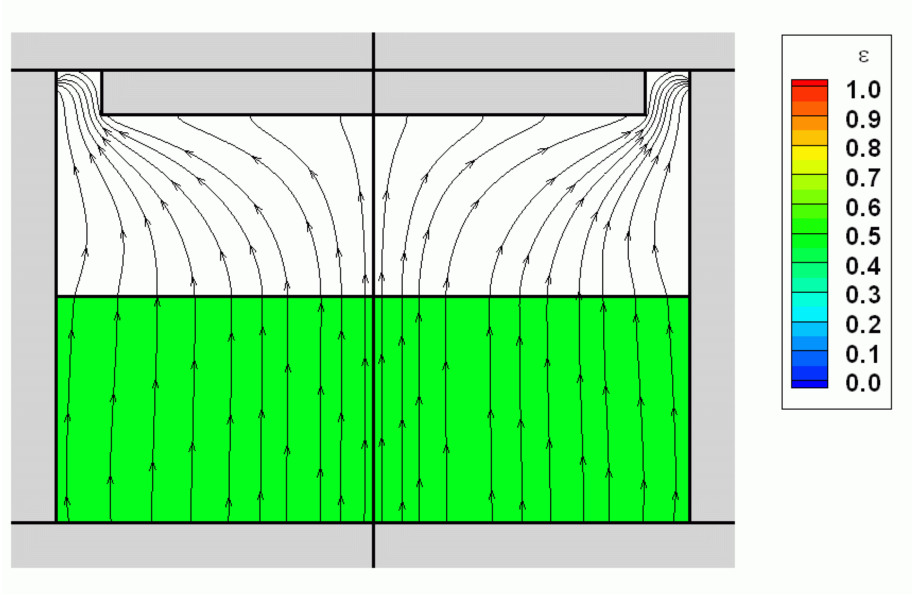

Porosity distribution and
the flow pattern
in the source and gas chamber

t = 2 h

Initial porosity = 0.5

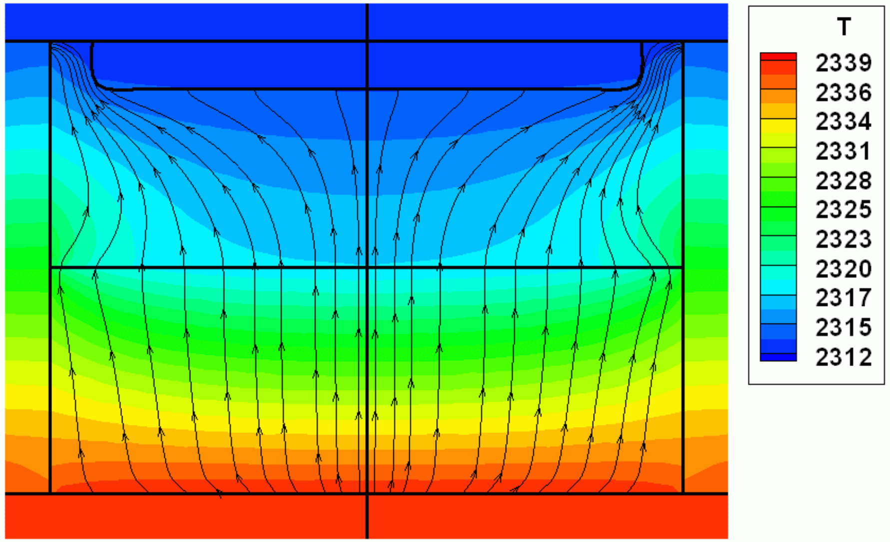

Temperature distribution and the flow pattern in the source and gas chamber

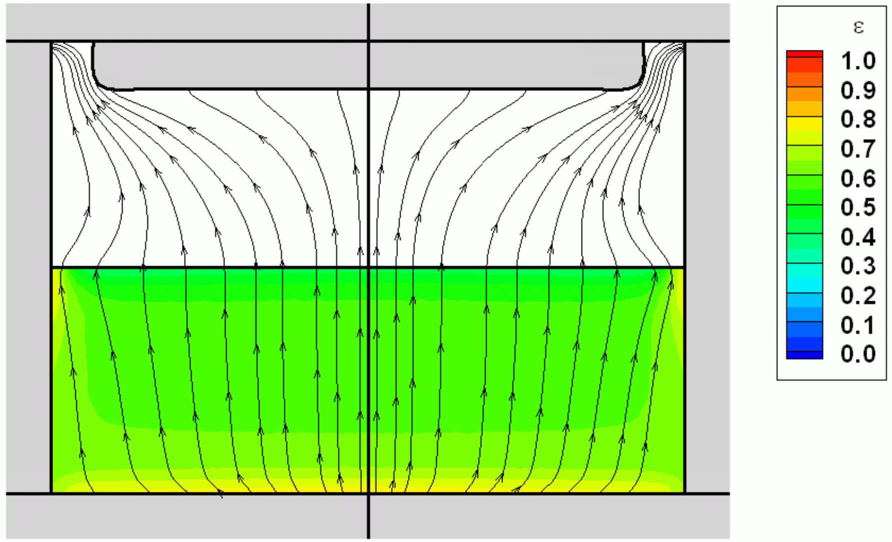

Porosity distribution and the flow pattern in the source and gas chamber

t = 5 h

Initial porosity = 0.5

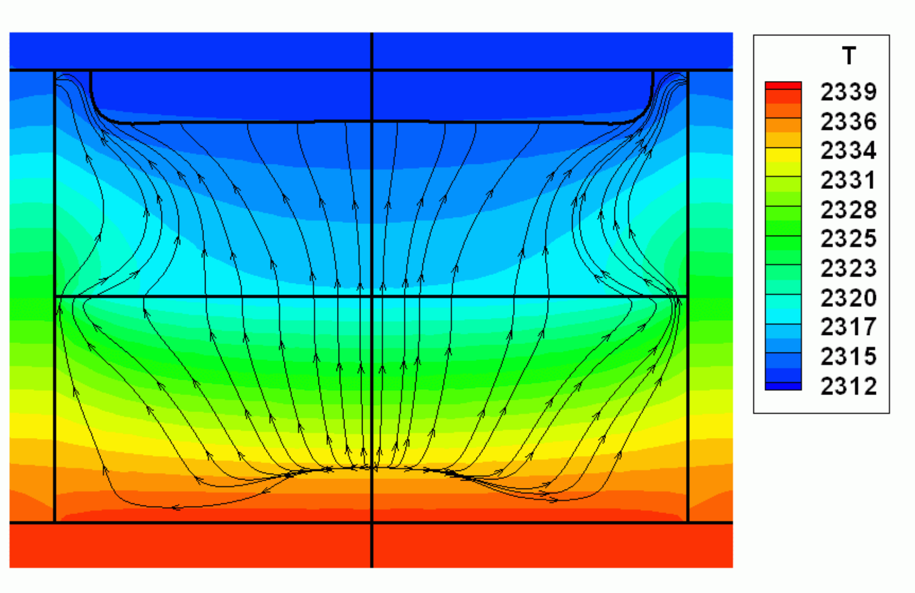

Temperature distribution and the
flow pattern
in the source and gas chamber

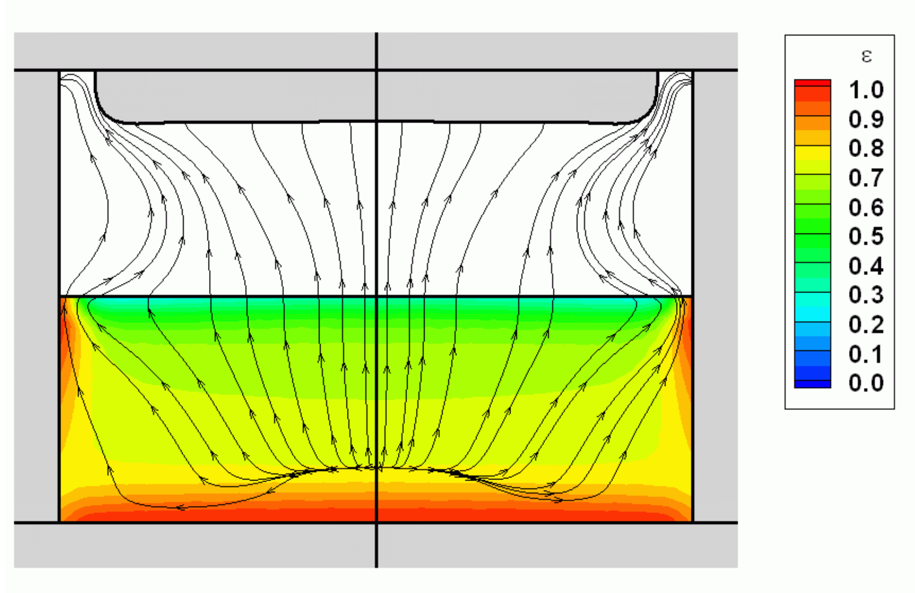

Porosity distribution and
the flow pattern
in the source and gas chamber

Modeling of Species Mass Transport in AlN Porous Source

t = 10 h

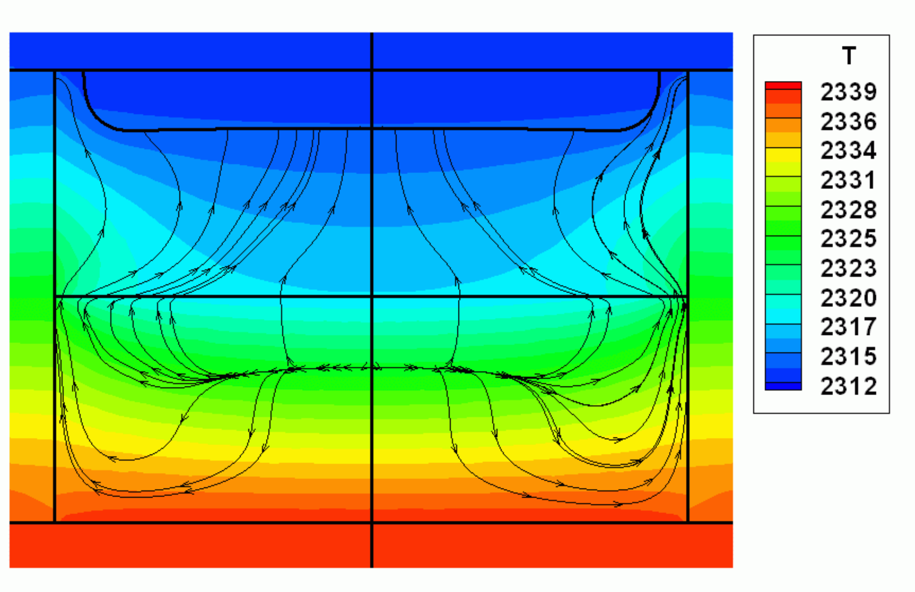

Temperature distribution and the
flow pattern
in the source and gas chamber

Initial porosity = 0.5

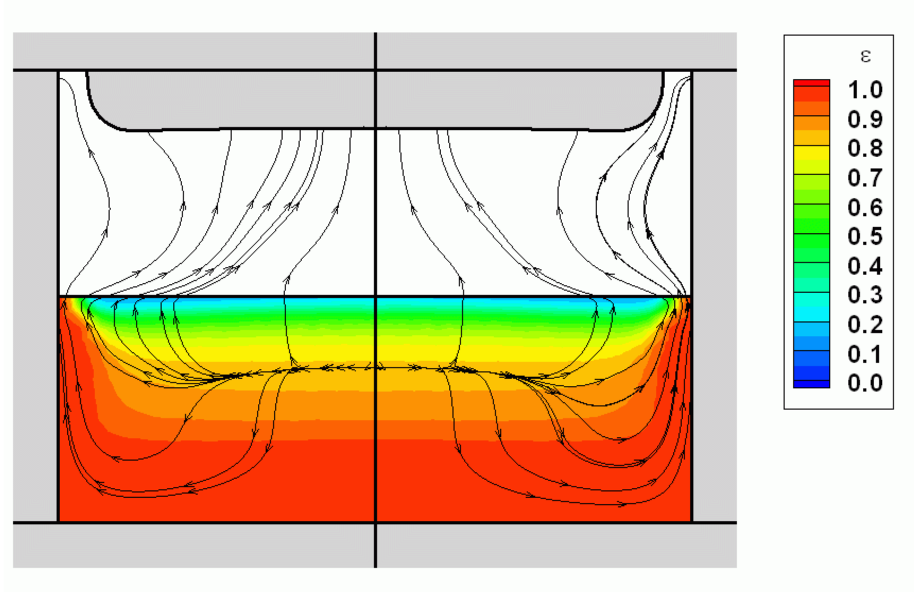

Porosity distribution and
the flow pattern
in the source and gas chamber

t = 20 h

Initial porosity = 0.5

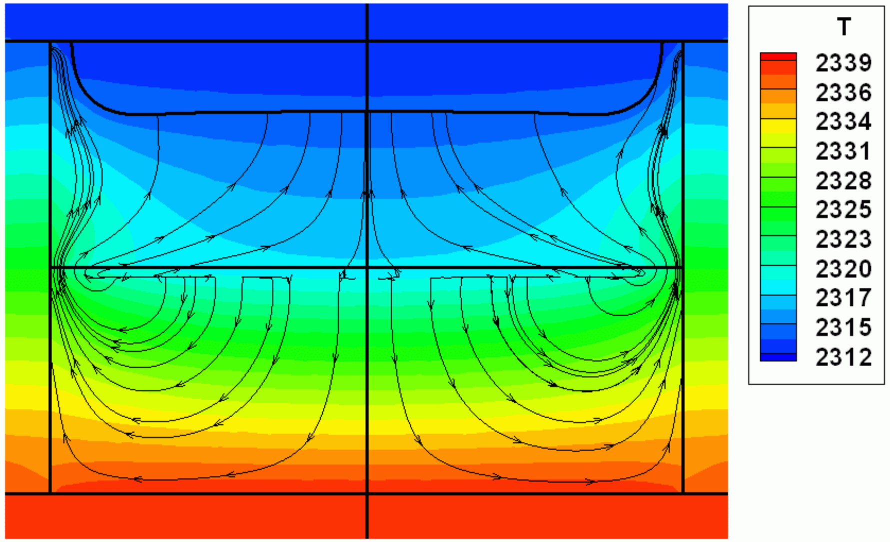

Temperature distribution and the flow pattern in the source and gas chamber

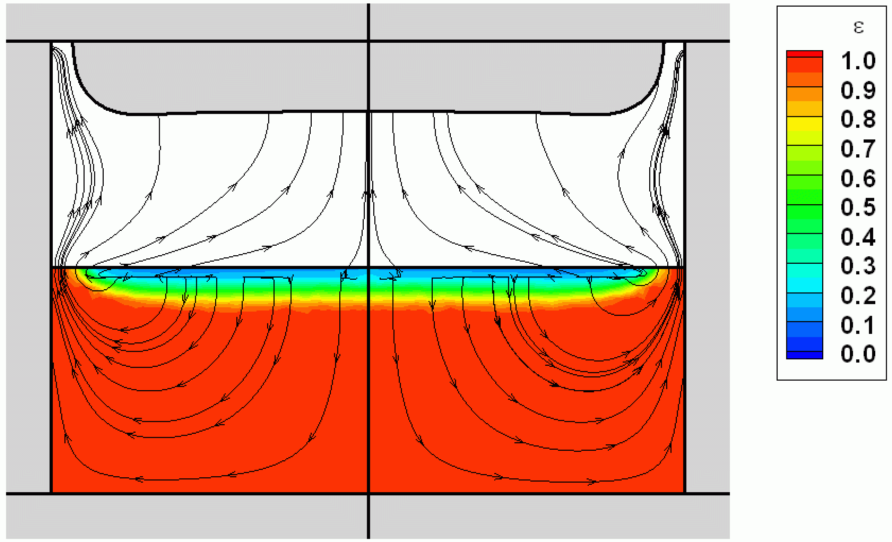

Porosity distribution and the flow pattern in the source and gas chamber

Main Results:

- ✓ Zone of active sublimation in the porous source is initially localized at the hot area and moves into the source bulk while the hot zones completely sublime
- ✓ Reduced porosity zones are formed in relatively cold regions

Analysis of Thermal Elastic Stress and Dislocation Evolution. Basic Features

- Finite-element analysis of the thermal elastic stress in AlN crystals

- Evaluation of the density of the dislocations gliding in the basal (0001) plane on the assumption of a full stress relaxation due to plastic deformation (S.Yu. Karpov et al., *J.Cryst. Growth* 211 (2000) 347)

Analysis of Thermal Elastic Stress

t = 0

Temperature

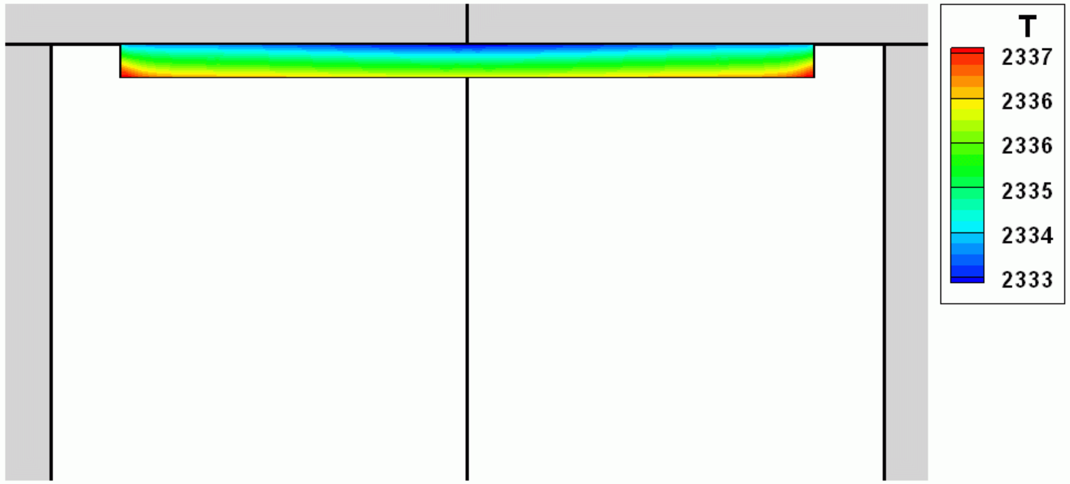

Applied Stress

(Magnitude of σ_{rz} Stress Component)

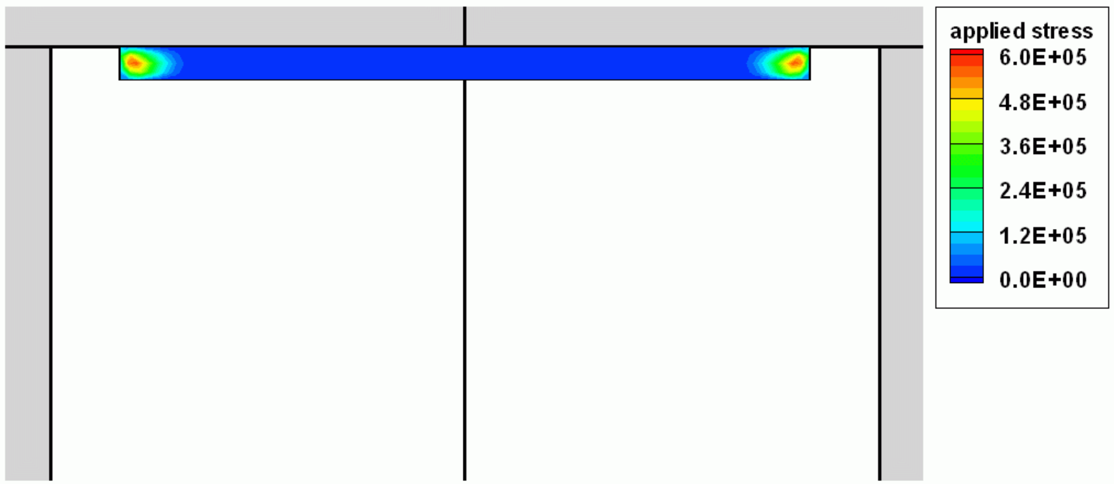

Analysis of Thermal Elastic Stress

t = 10

Temperature

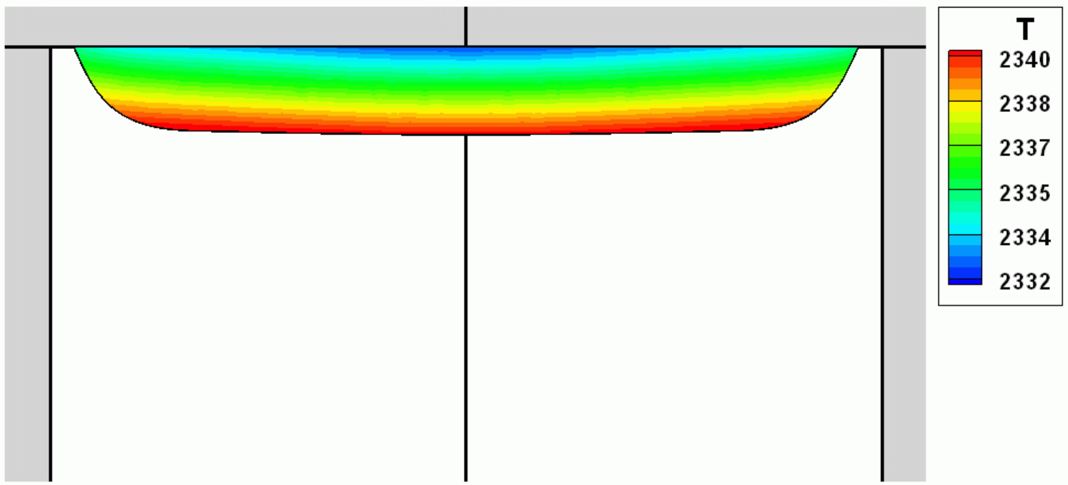

Applied Stress

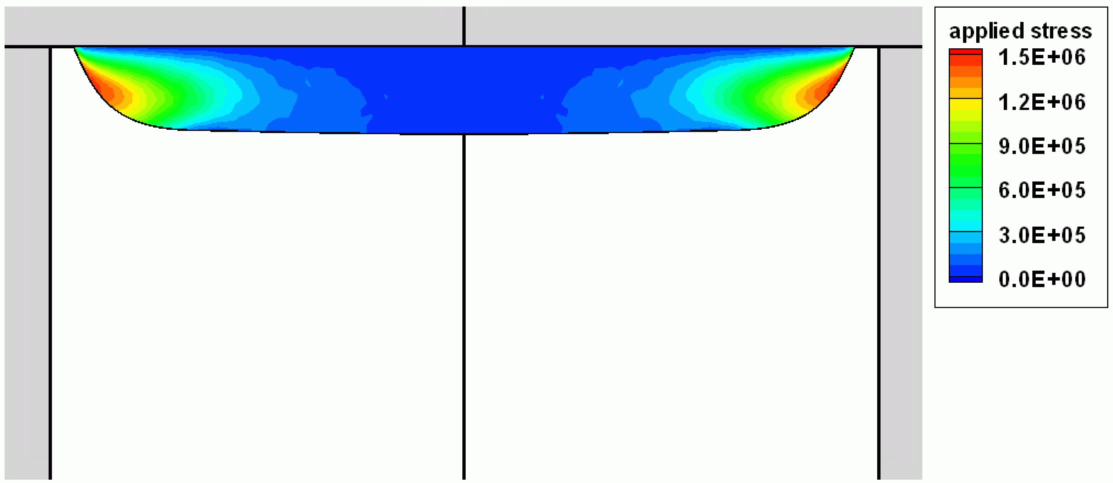

Analysis of Thermal Elastic Stress

t = 30

Temperature

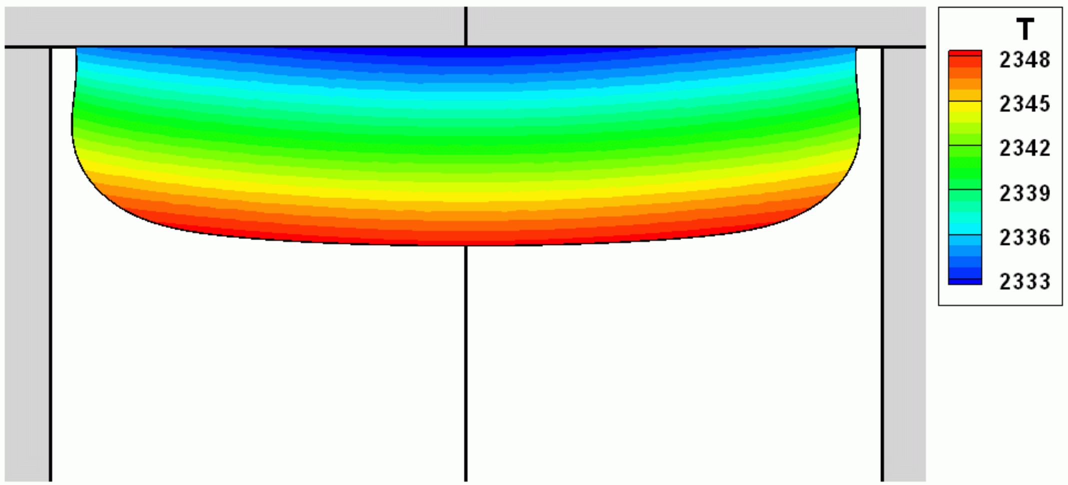

Applied Stress

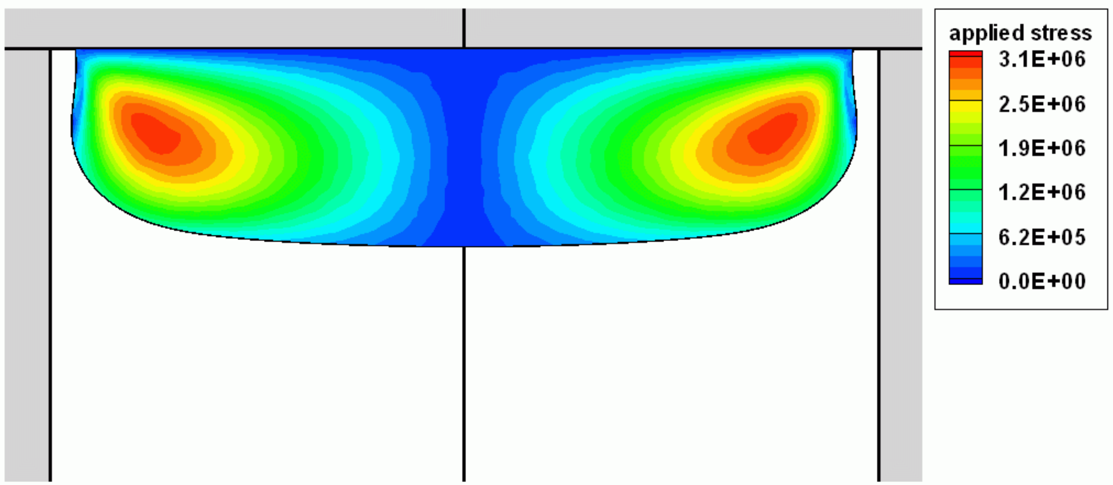

Analysis of Thermal Elastic Stress

t = 50

Temperature

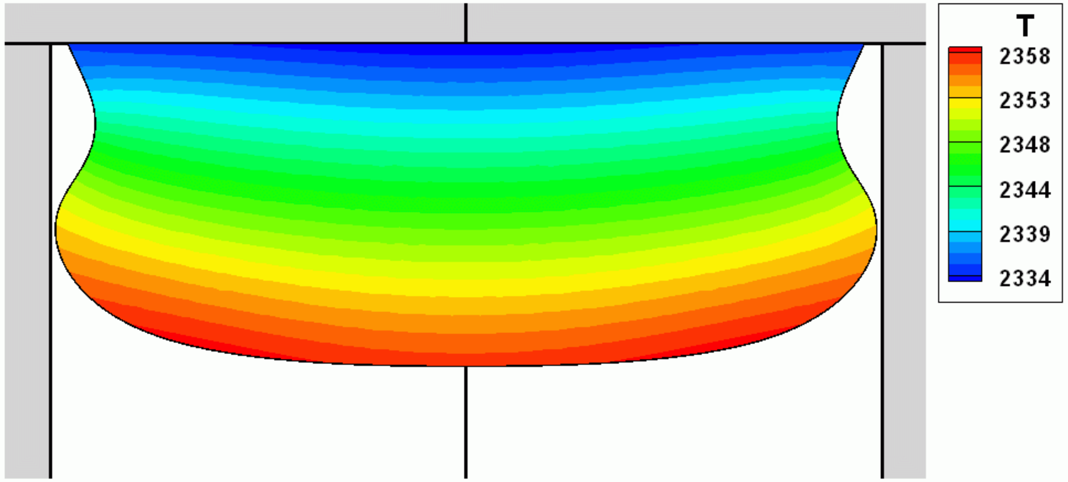

Applied Stress

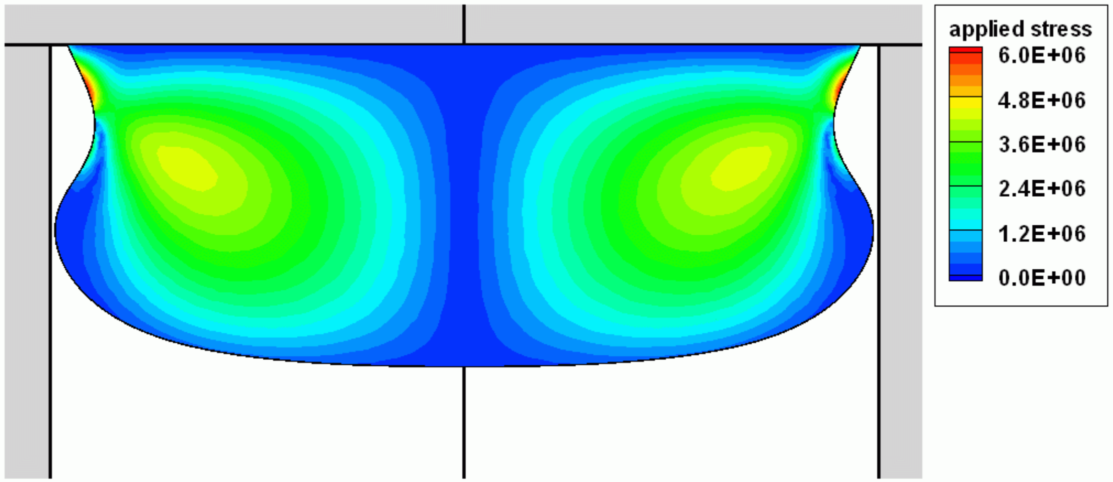

Analysis of Threading Dislocation Dynamics. Principal Slip Systems in a Hexagonal Crystal

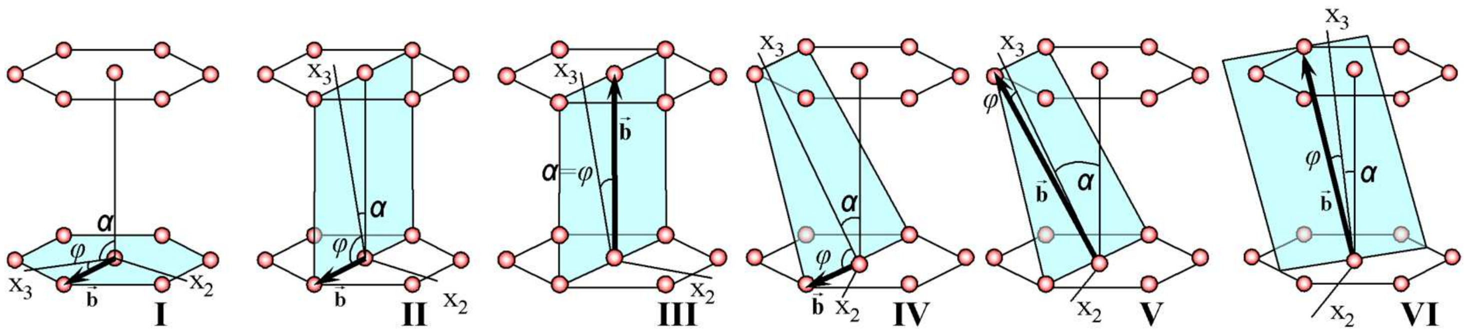

I – $(0001)\langle 1\bar{2}10\rangle$
II – $\{10\bar{1}0\}\langle 1\bar{2}10\rangle$
III – $\{10\bar{1}0\}\langle 0001\rangle$
IV – $\{10\bar{1}1\}\langle 1\bar{2}10\rangle$
V – $\{10\bar{1}1\}\langle \bar{1}\bar{1}23\rangle$
VI – $\{\bar{2}112\}\langle 2\bar{1}\bar{1}3\rangle$

Virtual Reactor predicts propagation of dislocations of **II** (prismatic) and of **III** (screw) type frequently observed in the growing bulk crystal

Analysis of Threading Dislocation Dynamics. Prismatic Dislocations

$$\{10\bar{1}0\} < 1\bar{2}10 >$$

Dislocation traces in bulk crystal growth

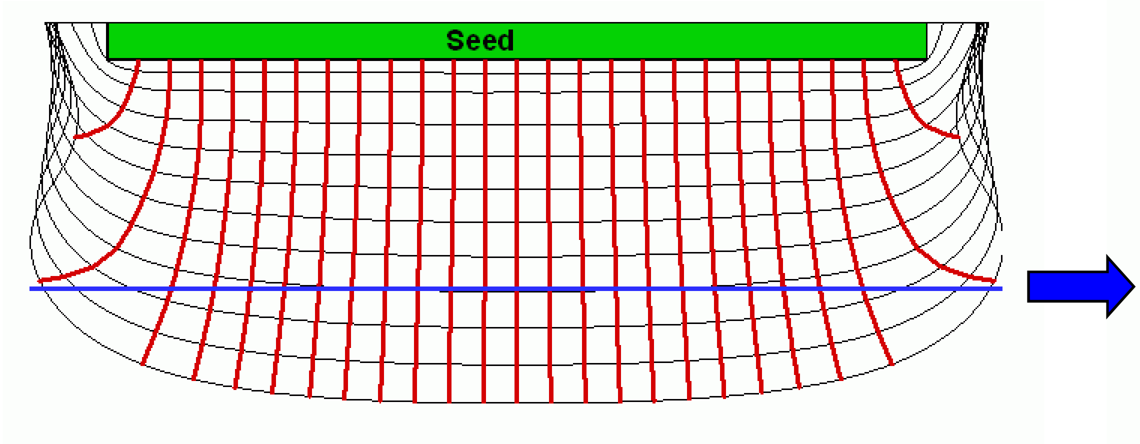

Wafer mapping

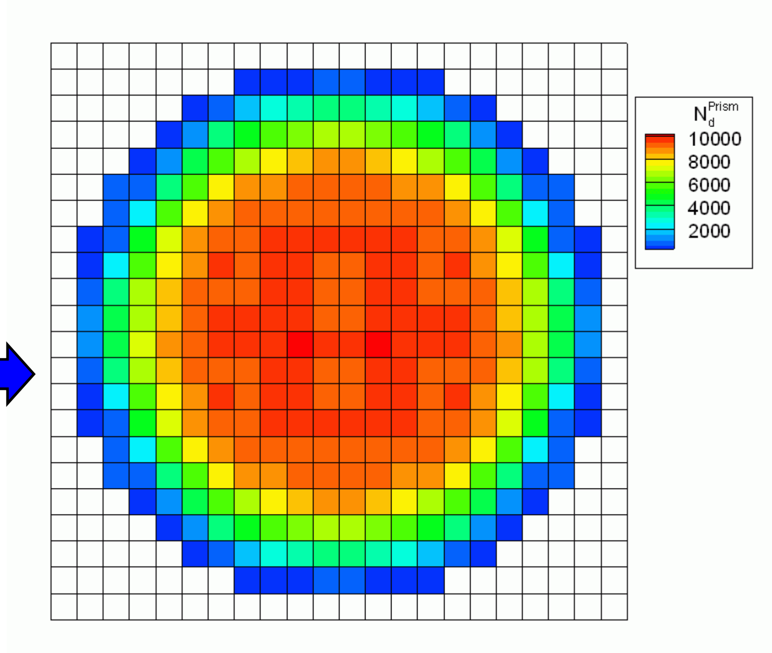

Dislocation density, cm^{-2}

Analysis of Threading Dislocation Dynamics.
Screw Dislocations

$$\{10\bar{1}0\} < 0001 >$$

Dislocation traces in bulk crystal growth

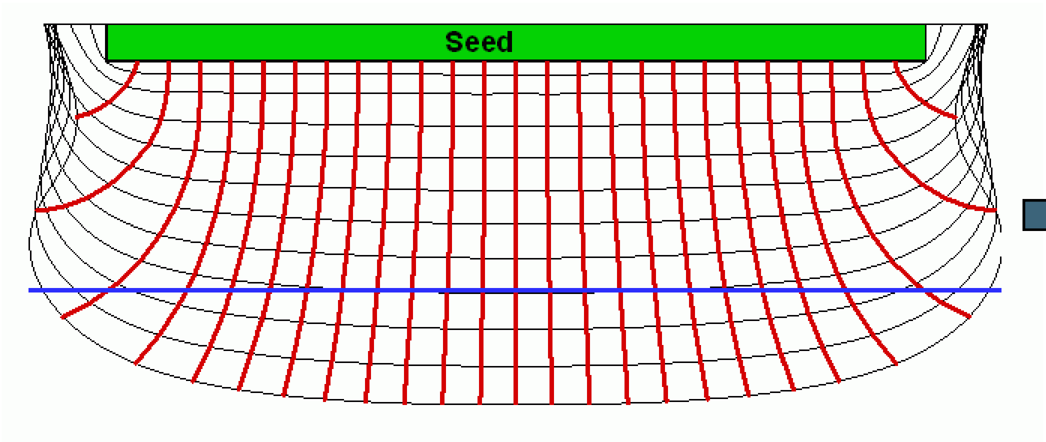

Wafer mapping

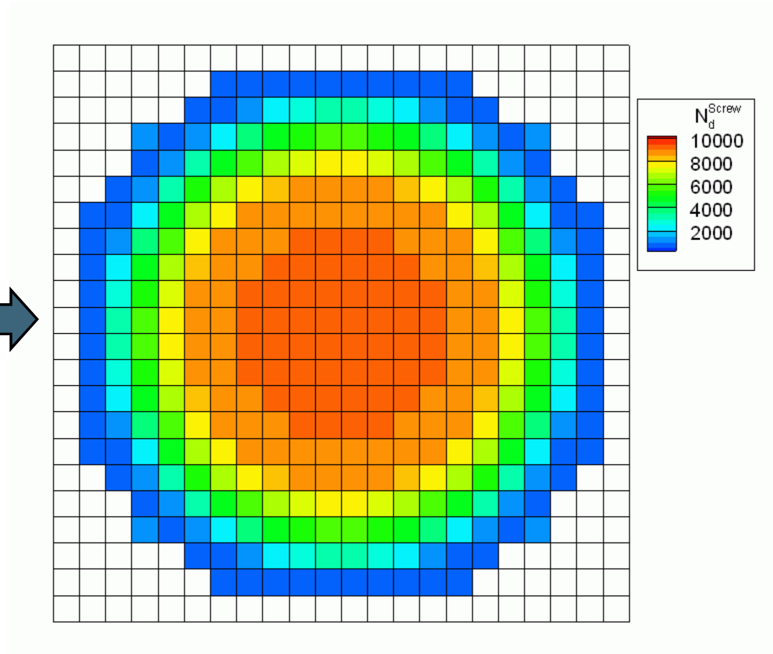

Dislocation density, cm^{-2}

STR

Some VR users in Europe

SiCrystal AG

НИТРИДНЫЕ КРИСТАЛЛЫ

POLITECHNIKA WARSZAWSKA
WARSAW UNIVERSITY OF TECHNOLOGY

LINKÖPINGS UNIVERSITET

Физико-технический институт им.А.Ф.Иоффе

NORSTEL

Freiberger Compound Materials GmbH

IKZ

FAU FRIEDRICH-ALEXANDER UNIVERSITÄT ERLANGEN-NÜRNBERG

Санкт-Петербургский государственный электротехнический университет «ЛЭТИ»
1886

1899

FBH Leibniz Ferdinand-Braun-Institut

ОАО Государственный завод ПУЛЬСАР

ВЕГА
ОТКРЫТОЕ АКЦИОНЕРНОЕ ОБЩЕСТВО «КОНЦЕРН РАДИОСТРОЕНИЯ «ВЕГА»
JOINT-STOCK COMPANY «RADIO ENGINEERING CORPORATION «VEGA»

Some VR users in South-East Asia

Nagoya University

The Nobel Prize in Physics 2014

Prof. Hiroshi Amano

NIPPON STEEL

Fujikura

SICCAS Since 1928

DONG-EUI UNIVERSITY

山东大学 SHANDONG UNIVERSITY

CETC

BRIDGESTONE

漢民 Hermes Epitek

ShinEtsu

哈爾濱工業大學 HARBIN INSTITUTE OF TECHNOLOGY

KICET KOREA INSTITUTE OF CERAMIC ENGINEERING AND TECHNOLOGY

SHOWA DENKO

SUMITOMO ELECTRIC

CRIEPI Central Research Institute of Electric Power Industry

MEIJO UNIVERSITY FOUNDED 1926 NAGOYA JAPAN

SKC

DENSO

OCI

西安理工大学 XI'AN UNIVERSITY OF TECHNOLOGY

Institute of Semiconductors Chinese Academy of Sciences

Publications

M.V. Averyanova, S.Yu. Karpov, Yu.N. Makarov, M.S. Ramm, R.A. Talalaev, Theoretical model for analysis and optimization of group III-nitrides growth by molecular beam epitaxy. MRS Internet Journal of Nitride Semiconductor Research 1, Art.31, (1996)

M.V. Averyanova, I.N. Przhevalskii, S.Yu. Karpov, Yu.N. Makarov, M.S. Ramm, R.A. Talalaev, Analysis of vaporization kinetics of group-III nitrides. Materials Science and Engineering B43, p.167-171, (1997)

S.Yu. Karpov, Yu.N. Makarov, M.S. Ramm, The role of gaseous species in group-III nitride growth. MRS Internet Journal of Nitride Semiconductor Research 2, Art.45, (1997)

S.Yu. Karpov, Yu.N. Makarov, M.S. Ramm, R.A. Talalaev, Control of SiC growth and graphitization in sublimation sandwich system. Materials Science and Engineering B46, p.340-344, (1997)

S.Yu. Karpov, D.V. Zimina, Yu.N. Makarov, E.N. Mokhov, A.D. Roenkov, M.G. Ramm, Yu.A. Vodakov, Sublimation growth of AlN in vacuum and in a gas atmosphere. Physica Status Solidi (a) 176, p.435-438, (1999)

I.A. Zhmakin, A.V. Kulik, S.Yu. Karpov, S.E. Demina, M.S. Ramm, Yu.N. Makarov, Evolution of thermoelastic strain and dislocation density during sublimation growth of silicon carbide. Diamond and Related Materials 9, p.446-451, (2000)

Publications (continued)

A.S. Segal, S.Yu. Karpov, Yu.N. Makarov, E.N. Mokhov, A.D. Roenkov, M.G. Ramm, Yu.A. Vodakov, On mechanisms of sublimation growth of AlN bulk crystals. Journal of Crystal Growth 211, p.68-72, (2000)

M.V. Bogdanov, A.O. Galyukov, S.Yu. Karpov, A.V. Kulik, S.K. Kochuguev, D.Kh. Ofengeim, A.V. Tsirulnikov, M.S. Ramm, A.I. Zhmakin, Yu.N. Makarov, Virtual reactor as a new tool for modeling and optimization of SiC bulk crystal growth. Journal of Crystal Growth 225, p.307-311, (2001)

M.V. Bogdanov, A.O. Galyukov, S.Yu. Karpov, A.V. Kulik, S.K. Kochuguev, D.Kh. Ofengeim, A.V. Tsirulnikov, I.A. Zhmakin, A.E. Komissarov, O.V. Bord, M.S. Ramm, A.I. Zhmakin, Yu.N. Makarov, Virtual reactor: a new tool for SiC bulk crystal growth study and optimization. Materials Science Forum 353-356, p.57-60, (2001)

S.Yu. Karpov, A.V. Kulik, M.S. Ramm, E.N. Mokhov, A.D. Roenkov, Yu.A. Vodakov, Yu.N. Makarov, AlN crystal growth by sublimation technique. Materials Science Forum 353-356, p.779-782, (2001)

S.Yu. Karpov, A.V. Kulik, A.S. Segal, M.S. Ramm, Yu.N. Makarov, Effect of reactive ambient on AlN sublimation growth. Physica Status Solidi (a) 188, p.763-767, (2001)

M.V. Bogdanov, S.Yu. Karpov, A.V. Kulik, M.S. Ramm, Yu.N. Makarov, R. Schlesser, R.F. Dalmau, Z. Sitar, Experimental and theoretical analysis of heat and mass transport in the system for AlN bulk crystal growth. Materials Research Society Symposium Proceedings 743, p.L3.33, (2003)

Publications (continued)

M.V. Bogdanov, S.E. Demina, S.Yu. Karpov, A.V. Kulik, M.S. Ramm, Yu.N. Makarov, Advances in modeling of wide-bandgap bulk crystal growth, *Cryst. Res. Technol*. 38, p.237-249, (2003)

S.Yu. Karpov, A.V. Kulik, I.N. Przhevalskii, M.S. Ramm, and Yu.N. Makarov Role of oxygen in AlN sublimation growth, *Phys. Stat. Sol. (c)* 0(7), p.1989-1992, (2003)

M.V. Bogdanov, D.Kh. Ofengeim, A.I. Zhmakin, Industrial Challenges for Numerical Simulation of Crystal Growth, *Centr. Eur. Jour. Phys*. 2 (1), p.183-203, (2004).

A.V. Kulik, M.V. Bogdanov, S.Yu. Karpov, M.S. Ramm, Yu.N. Makarov, Theoretical Analysis of the Mass Transport in the Powder Charge in Long-Term Bulk SiC Growth, *Mat. Sci. Forum* 457-460, p.67-70, (2004).

A.K. Semennikov, S.Yu. Karpov, M.S. Ramm, A.E. Romanov, and Yu.N. Makarov, Analysis of threading dislocations in wide-bandgap hexagonal semiconductors by energetic approach, *Materials Science Forum* 457-460, p.383-386, (2004).

E. Mokhov, S. Smirnov, A. Segal, D. Bazarevsky, Yu. Makarov, M. Ramm, and H. Helava. Experimental and Theoretical Analysis of Sublimation Growth of Bulk AlN Crystals. *Materials Science Forum* 457-460, p.1545-1548, (2004).

Conclusions

VR-PVT AlN™ is an effective tool for simulation of long-term sublimation growth of bulk AlN crystals

Any questions concerning Virtual Reactor software tools can be sent to
vr-support@str-soft.com

General presentation demonstrating capabilities of the Virtual Reactor software package and presentations demonstrating other editions of Virtual Reactor family, such as

- **VR-PVT SiC™**
- **HEpiGaNS™**
- **VR-CVD SiC™**

are available upon request